NASA TECHNICAL NOTE

NASA TN D-5019

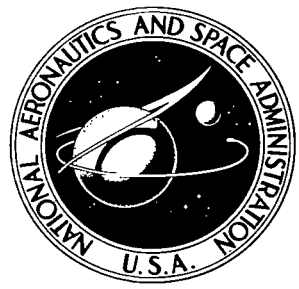

EXAMINATION OF OXIDE SCALES ON HEAT RESISTING ALLOYS

by Salvatore J. Grisaffe and Carl E. Lowell

Lewis Research Center
Cleveland, Ohio

NATIONAL AERONAUTICS AND SPACE ADMINISTRATION • WASHINGTON, D. C. • FEBRUARY 1969

EXAMINATION OF OXIDE SCALES ON HEAT RESISTING ALLOYS

By Salvatore J. Grisaffe and Carl E. Lowell

Lewis Research Center
Cleveland, Ohio

NATIONAL AERONAUTICS AND SPACE ADMINISTRATION

For sale by the Clearinghouse for Federal Scientific and Technical Information
Springfield, Virginia 22151 – CFSTI price $3.00

ABSTRACT

Twelve iron, nickel, and cobalt heat resisting alloys were cyclic furnace oxidation tested at from 1400° to 2200° F (1033 to 1478 K) for from 4 to 600 hours. Retained oxide scales and spall were identified using X-ray diffraction combined with X-ray fluorescence analysis. Metallography clarified scale growth sequences. After 600 hours at 2000° F (1366 K), the condition most studied, the best oxidation resistance, as reflected by weight change and spall weight, was exhibited by alloys forming single oxide scales of Al_2O_3 or Cr_2O_3. For alloys that developed multioxide scales, spinel constituent composition or lattice parameter did not correlate with oxidation resistance.

EXAMINATION OF OXIDE SCALES ON HEAT RESISTING ALLOYS

by Salvatore J. Grisaffe and Carl E. Lowell

Lewis Research Center

SUMMARY

Twelve commercial heat resisting alloys - iron, nickel, and cobalt based - were cyclic furnace oxidation tested in air for NASA Lewis Research Center by a commercial laboratory. Exposure temperatures ranged from 1400° to 2200° F (1033 to 1478 K), while time ranged from 4 to 600 hours. Samples of both the oxidized sheet specimens and oxide spall were subsequently sent to Lewis for analysis. Data from X-ray diffraction and X-ray fluorescence studies were combined to identify the oxide constituents. Spinels were identified from lattice parameter and element intensity information assuming Vegard's law to hold for spinel solid solutions. Bright field and polarized light metallographic studies of specimen surfaces and cross sections further clarified the sequence of scale growth and the location of scale constituents.

Specimens exposed at 2000° F (1366 K) were most thoroughly studied. After 600 hours at this temperature, the alloys exhibiting the best oxidation resistance (Fe-Cr-Al types or TD-NiCr) had formed only a single oxide scale - either Al_2O_3 or Cr_2O_3. The other alloys generally formed multioxide scales containing Cr_2O_3 and a variety of spinels or other oxide crystal structures. There was no apparent correlation between either the spinel composition or spinel lattice parameter and the oxidation resistance of those alloys.

INTRODUCTION

Oxidation resistance at high temperatures is an important criterion in the evaluation of materials for airbreathing engines. However, the comparison of literature oxidation data, obtained by different researchers, is difficult since there are wide differences in testing and evaluation techniques. To provide more realistic comparisons, sheet specimens of 12 commercial heat resisting alloys were simultaneously tested in cyclic furnace oxidation for NASA Lewis Research Center (ref. 1) by an industrial laboratory. Such furnace tests were used as a preliminary screening procedure for selected heat resisting sheet materials. Subsequently, the most promising alloys were further oxidation

tested in wire form by the same investigators. Such tests, supplemented with mechanical property evaluation, were used to determine the potential of the various materials for wire wrapped and sintered porous structures. Structures of this type hold promise as transpirational cooled turbine blades.

The 12 alloys originally tested in sheet form included representatives from iron, nickel, and cobalt based chemistries. Tests ranged from 4 to 600 hours at temperatures of from 1400° to 2200° F (1033 to 1478 K). Weight gain, spall weight, scale thickness, and depth of oxide penetration were among the data obtained. These data are necessary for a comparison of alloys. However, it is desirable to supplement such data with information regarding the oxide microstructure, composition, and morphology. To this end, samples from the oxidation specimens were examined at this Center. The results of that examination are reported here.

The objective of these studies on oxide scales was to provide more basic information about the scales formed on the alloy sheet and to try to correlate this information with alloy oxidation behavior. The primary investigative methods used were metallography, X-ray diffraction (XRD), and X-ray fluorescence (XRF) analysis.

Although cursory examinations were given to all of the time-temperature combinations, emphasis was placed on the 600-hour tests at 2000° F (1366 K). This temperature was considered to be an upper limit to useful alloy strength as well as the level above which serious oxidation could be anticipated for most alloys.

MATERIALS AND MATERIAL HISTORY

The 12 alloys examined can be divided into three main groups as shown in the following table:

Iron base	Nickel base	Cobalt base
N-155 GE 1541 HS-875	Nickel and nickel-chromium type	L-605
	TD-Ni TD-NiCr Chromel A DH242 Bendel	
	Complex nickel-base alloys	
	Hastelloy X Udimet 500 RA 333	

Table I (ref. 1) lists each alloy along with its chemical analysis by both the alloy vendor and by an independent laboratory. In some instances, notable differences exist between the two analyses. For example, differences can be noted in the carbon content in TD-Ni, TD-NiCr, and Hastelloy X; the silicon content in Chromel A and GE 1541; the manganese content in Chromel A and DH242; the sulfur content in TD-Ni and L-605; and the iron content in Udimet 500. These differences may reflect variations in alloy homogeneity as well as differences in analytical techniques.

Prior to the oxidation test, the contractor gave each material two separate hydrogen [dew point, -60° F (223 K)] anneals for 4 hours each at 2100° F (1422 K). These anneals simulate the sintering treatment used to fabricate transpirational cooled blades.

Sheet specimens, 6 by 1/2 by 0.050 inches (15.2 by 1.27 by 0.127 cm) were abraded through #360 aluminum oxide grit by the contractor to produce final surface roughnesses ranging from 10 to 12 microns root mean square. These large specimens were then individually inserted into 7-inch- (17.8-cm-) long zircon "test tubes" having an internal diameter of 3/4 inch (1.91 cm). (Specimens contacted the tubes at only four points.) The test tubes were drilled with four 1/8-inch- (0.31-cm-) diameter holes, evenly spaced at 90° angles, located 1 inch (2.54 cm) from both the top and bottom. These holes allowed free circulation of air. Furthermore, each tube was covered with a zircon cap to retain spall and prevent furnace lining material from contaminating the collected spall.

Ten specimens of each alloy were cyclic oxidation tested. The cycle times were 4 hours for the first exposure followed by 12, 48, and 36 hours to give total exposure times of 4, 16, 64, and 100 hours. Thereafter, 100-hour cycles were used to a total of 600 hours. Exposure temperatures were 1400°, 1600°, 1800°, and 2000° F (1033, 1144, 1254, and 1366 K), with limited tests at 2100° and 2200° F (1422 and 1478 K). After each exposure cycle, specimens were removed from the furnace and air cooled. All specimens were weighed and then returned to their crucibles. After each exposure, however, at least one specimen of each alloy was removed from further testing. The contractor then cut small pieces, approximately 1 by 1/2 inch (2.54 by 1.27 cm) from the ends of the large 6- by 1/2-inch (15.2- by 1.27-cm) specimens. Each of these small pieces was sealed in a plastic envelope. Any spall from that exposure was emptied from the crucible and was also sealed in a similar envelope. These envelopes were sent to Lewis for scale analysis.

EXPERIMENTAL PROCEDURE

SAMPLE SELECTION

Selected scales and spalled oxides formed at all of the temperatures and times were studied to establish growth and compositional trends. The main emphasis, however, was given to the long-time 2000° F (1366 K) specimens with the others providing information on the trends. Since no samples of the unexposed metals were available, 4-hour 1400° F (1033 K) samples were used as representative of the original material. At that level of exposure, only slight surface tarnishes had formed.

X-RAY FLUORESCENCE AND DIFFRACTION

XRF scans were obtained from the oxide scales in situ. The X-ray tube used to generate white radiation to obtain the excitation of each element's characteristic radiation, had a gold target. A lithium fluoride (LiF) crystal and a proportional counter were used for separation and detection of the emitted X-rays. For each scale analysis, a continuous chart record was made of the emitted spectrum to determine qualitatively which elements were present. Then, the intensity of each element's characteristic K alpha radiation was recorded by returning to the exact wavelengths and measuring the counts for a constant time of 30 seconds. For heavy elements such as tungsten (W), with short K alpha wavelengths, the intensity of the L alpha radiation was measured. Elements whose atomic numbers are 22 (i.e., Ti) and above can be detected and measured with this technique. Those with atomic numbers below 22 require a helium or vacuum path fluorescence unit and thus were not measured in this investigation. In XRF analysis, the position of the K absorbtion edge of one element in relation to the K alpha or L alpha of a second element can decrease the measured radiation intensity fluoresced from the second element. Since all of these absorption edges contribute to the way in which radiation is absorbed by the oxide scale, these intensity measurements must be viewed as only semiquantitative and thus and ratios of these intensities can also be viewed as only semiquantitative.

A second factor also influences the semiquantitative nature of such XRF data. By examining the oxide scales in situ, some contribution of radiation fluoresced by the substrate can occur. Unfortunately, scraping the oxide from the substrate, while eliminating this objection, can also affect results. The effect is caused by the inability to remove all of the scale so that the more adherent portions may well have a different composition from that of the easily removed material.

Primarily, then, the in situ approach was used with the drawbacks kept in mind. Trends in elemental concentration in the scale were easily observed. With thicker scales as with the spalls, the substrate contribution was negligible. As a check, however, some scales were analyzed both in situ and as scraped.

XRD analyses were made using 114.6-millimeter-diameter Debye powder cameras of the Straumanis film loading type. Cobalt K alpha radiation was generally used for the iron and cobalt alloys. Copper K alpha radiation was used for the nickel-base alloys. Samples for diffraction were prepared by removing the oxides from the substrates with the aid of a vibrating diamond engraving tool. Removal was dictated by the generally weak patterns obtained from the in situ oxides on the film. Besides the camera work, diffractometer scans were also run in some cases on the in situ oxide scales. In general, these failed to detect the minor oxide phases present.

In order to even approach the exact identification of oxide scales, both the XRF and XRD data are required. The XRD data provide only crystallographic information such as crystal structure and lattice constants. The XRF data supplement this with information as to which elements are present. Thus, many possible oxides can be ruled out but others still remain. Then the question of solutions of oxides must also be considered. In the case of simple oxides, for example, on an alloy containing both cobalt and nickel, the determination of only one oxide with a sodium chloride (NaCl) structure and with a lattice constant close to that of cobalt oxide (CoO) but with significant nickel found in the XRF scans will be interpreted to mean cobalt monoxide with nickel in solid solution. Iron or manganese could also substitute in such an oxide. Another example is the identification of chromic oxide (Cr_2O_3). This oxide is isomorphous with ferric oxide (Fe_2O_3) and aluminum oxide (Al_2O_3) and these oxides are mutually soluble. If the lattice constants are close to that of Cr_2O_3 and if only minor traces of iron or aluminum are found in the scale, then the oxide will be identified as Cr_2O_3. The fact that this is a simplification of the actual situation must be remembered by the reader.

The situation with spinels is even more complex. Spinel is a generic term for more complex cubic oxides of the composition RR'_2O_4. The R may be, among others, cobalt (Co), nickel (Ni), manganese (Mn), iron (Fe), magnesium (Mg), titanium (Ti), lithium (Li), and copper (Cu). R' may be, among others, Mn, Fe, chromium (Cr), Co, and aluminum (Al). Spinels may exist where the valence ratio of R:R' is 2:3, 4:2, and 6:1. Many spinels are mutually soluble in wide proportions and thus more than one R or R' element may be found at any appropriate crystal lattice site, for example, $(Ni, Fe)(Mn, Cr)_2O_4$. (For further background information on spinels see refs. 2 and 3.) This situation makes XRD analysis difficult - particularly in the presence of other oxide phases. The problem is related to the similarity in both the spacings and relative intensities of the diffraction lines. There is not sufficient difference in many cases to uniquely iden-

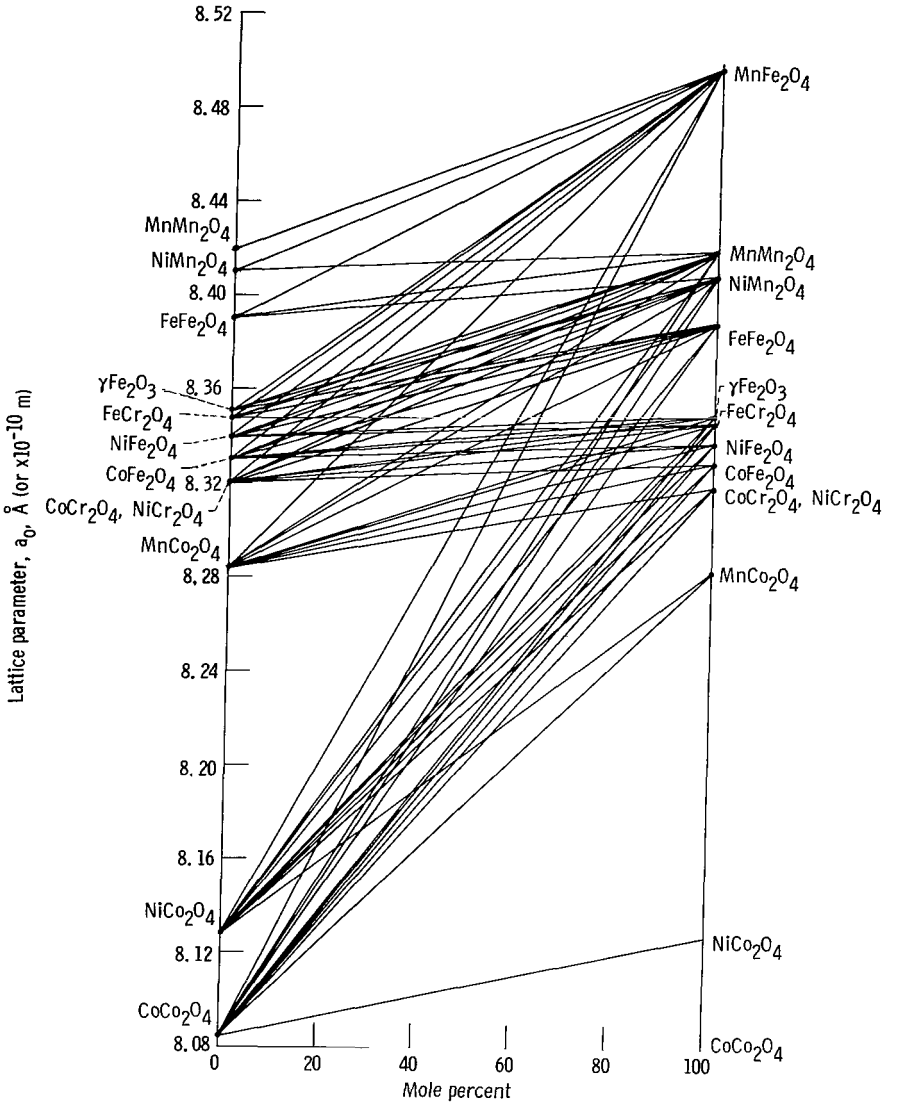

Figure 1. - Lattice parameter plotted against mole percent of spinel solutions.

tify the specific spinel present. For this reason, reliance must again be placed on a combination of lattice parameter and XRF data. Figure 1, containing lattice parameter data from reference 4, shows the effect of binary solid solutioning on the lattice parameters of various spinel phases assuming complete solid solubility and an adherence to Vegard's Law. To minimize the complexity of the diagram, only the spinels containing transition metals are shown. Since combinations of more than two spinels are possible and, in fact, common, difficulties in analysis are easy to perceive. Figure 1 was used as an aid in the interpreting of the XRD and XRF data obtained on spinels in this study.

An example of the determination of a spinel composition using the lattice parameter a_o data from diffraction, the fluorescence information, and figure 1 may be helpful to the reader. The spall from Udimet 500 after 600 hours at 2000° F (1366 K) had a spinel pattern with an a_o of 8.31±0.02 Å (or $\times 10^{-10}$ m) as the major phase (see table XII(a)). The fluorescence data indicated high chromium, cobalt, and nickel (see table XII(b)). Referring to figure 1, it can be seen that spinels with such a lattice constant and composition fit either $NiCr_2O_4$ or $CoCr_2O_4$. Thus, this phase would be identified as a solid solution of the two compounds - $(Ni, Co)Cr_2O_4$. In the case of a minor phase spinel, such predictions, of course, become more speculative.

METALLOGRAPHIC ANALYSIS

Scales on the 1/2- by 1-inch (1.27- by 2.54-cm) surfaces of selected oxidized materials were examined and photographed in situ at an angle of 90° to the surface. Magnifications employed ranged from 5 to 50 times. This procedure allowed observation of the gross structural characteristics of the scales. By examining these specimens under both bright field and polarized light on sequences involving more time at a fixed temperature or at the same time at different temperatures, scale growth patterns could be deduced.

Standard metallographic analyses of mounted and polished specimen cross sections was also conducted under both bright field and polarized light illumination. Magnifications employed included 250 and 500 times. Both the oxide scale and the metal scale interface were examined in the as polished condition. Subsequently, samples were etched to study substrate microstructural changes.

RESULTS

The weight gain and spall weight data for 600-hour 2000° F (1366 K) furnace air exposures, obtained in reference 1, are presented for completeness in table II. The metallographic analyses of specimen surfaces and cross sections are given in figures 2 to 7. The XRD and XRF data are combined for each alloy in tables III to XIV. The XRF data in these tables are presented both as actual element intensities and as the ratios of individual element intensity to those of the major alloy constituent.

IRON-BASE ALLOYS

N-155

N-155 is one of the very early high-temperature alloys and is the least oxidation resistant of all of the 12 alloys tested in reference 1. After 600 hours at 2000° F (1366 K), this alloy gained 45 milligrams per square centimeter - about 45 times that of the other two iron alloys. N-155 showed a total oxide spall weight of 250 milligrams per square centimeter. Both weight gain and spall weight are presented in table II. (Note that weight gain involves only the weight of oxygen picked up by the sample whereas spall weight involves the loss of both metal and oxygen in the form of spalled oxide. Thus, spall weight can be significantly greater than total weight gain.) The retained oxide thickness after the aforementioned exposure was 1.0 mil (0.001 in. or 25 μm (micrometers)).

The microstructure of a cross-sectioned specimen, showing both scale and substrate is presented in figure 2(a). After the 600-hour 2000° F (1366 K) exposure, this alloy retained about 1 mil (25 μm) of scale, but in many areas oxide penetration extended 4 mils below the surface. The retained scale had large green crystals, as seen under polarized light, indicating Cr_2O_3. These were interspersed with black regions which are indicative of a spinel. At the scale surface, a few red-brown spots were also seen under polarized light. These could represent another spinel. Beneath the scale, the substrate alloy was nonuniformly depleted in both substitutional elements as evidenced by the nonuniform, stepwise etching and in the fine carbide precipitate normally present. The blocky carbide phase persisted in the depleted zone and a few of the large particles were even observed in the oxide scale. The depletion zone extended about 2 mils (50 μm) below the surface. It contained a number of large voids, while many smaller voids were visible in the region directly beneath the depleted zone.

The metallographic analyses were confirmed by the XRD and XRF results (see table III). Table III(a) shows that a spinel phase was found by XRD in both the adherent scale and in the spall. The lattice constant of this spinel was between 8.32±0.02 and 8.34±0.02 Å. In addition, XRD confirmed the presence of Cr_2O_3 in the scale and detected some gamma Fe_2O_3 in the spall.

Table III(b) contains both the intensity data for the elements detected in counts per minute and these data normalized to the intensity of iron - the alloy base. XRF shows high chromium, nickel, cobalt, and iron in the scale and spall indicating, when combined with the lattice parameter data and the information in figure 1, that the spinel is probably close in chemistry to $(Ni, Co)(Cr, Fe)_2O_4$.

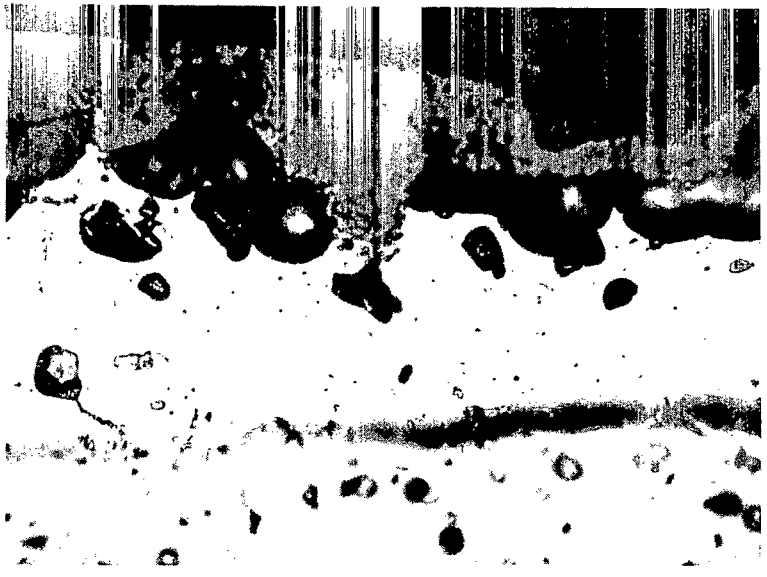

(a) N-155.

(b) GE 1541 (Fe-Cr-Al-Y).

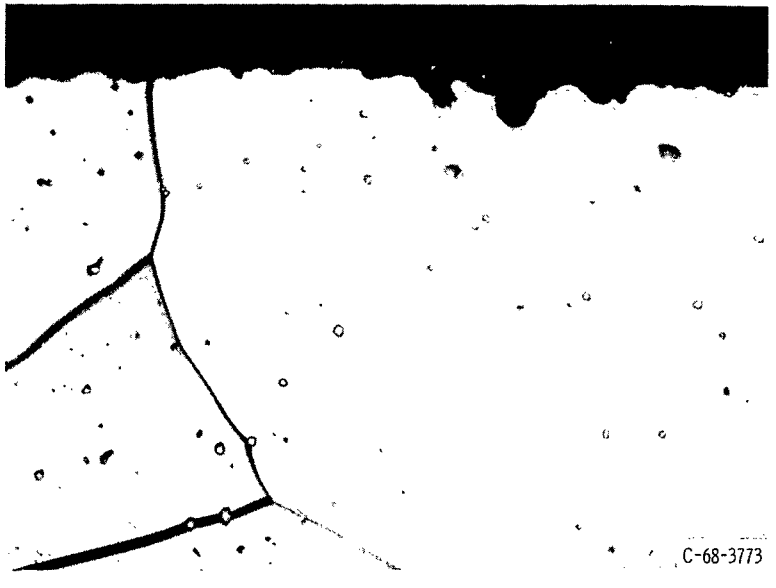

(c) HS-875 (Fe-Cr-Al).

Figure 2. - Iron-base alloys after 600 hours in air at 2000° F (1366 K). X500.

GE 1541

This Fe-15Cr-4Al-1Y alloy was one of the most oxidation resistant of all of the alloys studied. Table II shows that after 600 hours at 2000° F (1366 K), for example, the weight gain was only 1.1 milligrams per square centimeter while only a minute amount of scale spalled - 0.4 milligram per square centimeter. Similar weight gains were found over the same period at the same temperature for the continuous oxidation tests reported in reference 5 (p. 152).

Surface examination of this scale after a number of exposure times at several temperatures showed that oxidation initially occurred along surface scratches left from test specimen preparation. The thin scale, approximately 0.2 mil (5 μm) thick after 600 hours at 2000° F (1366 K), was pink when observed under polarized light indicating Al_2O_3 contaminated only slightly with chromium or iron impurities. This scale also showed planar faults at about 60° to the surface indicating some fracture of the scale due to thermal or growth stresses. These faults may be related to the scratches in the unoxidized specimens.

Figure 2(b), a photomicrograph of a scale-substrate cross section, shows the thin scale with preferential grain boundary oxidation occurring randomly in the substrate to a maximum depth of about 4 mils (100 μm). The substrate itself exhibited a large grain size. It contained a significant fraction of a globular phase reported to be YFe_9 (ref. 5, p. 147). This second phase appears to be preferentially depleted near the surface and oxidized grain boundaries.

XRD confirmed that, at all temperatures, the scale was primarily alpha Al_2O_3 (see table IV(a)). Progressive scraping on the 600-hour 1800° F (1254 K) specimen allowed the detection of some Cr_2O_3. None was detected in the retained scale or was observed metallographically in the 600-hour 2000° F (1366 K) specimen, however. XRF analysis (table IV(b)) showed little or no concentration of yttrium (Y) in the Al_2O_3 scale. No meaningful spall composition data were obtained for this alloy.

HS-875

Compared with GE 1541, HS-875 contains 25 weight percent chromium instead of 15 percent and no yttrium. The scales formed on this alloy were slightly thicker, in most cases, but the weight gain and spall weight were about the same, indicating less internal oxidation (which was confirmed on metallographic examination as shown in fig. 2(c)). After the 600-hour 2000° F (1366 K) test, this alloy gained only 0.9 milligram per square centimeter and had a spall loss of 0.5 milligram per square centimeter as shown in table II.

The scale formed at 2000° F (1366 K) appeared white under polarized light indicating fewer impurities in solution in Al_2O_3 than occurred in the case of the GE 1541 alloy. This scale also formed preferentially along surface scratches as can be seen from the two sequences of surface micrographs presented in figure 3. Figure 3(a) shows the formation of dark islands and light areas along the surface scratches after 4 hours at 1800° F (1254 K). After 600 hours at the same temperature (fig. 3(b)), the light oxide had substantially overgrown the dark patches. The 4-, 100-, and 600-hour sequences after a 2200° F (1478 K) exposure (figs. 3(c), (d), and (e)) also show this trend, but the dark areas are more rapidly overgrown by the white. The faults in the scale similar to that observed on GE 1541 can also be seen in the 100-hour (fig. 3(d)) and the 600-hour (fig. 3(e)) micrographs and may also be related to the surface scratches on the unoxidized specimen surface.

The metallographic examination of the oxide-substrate cross section after the 600-hour 2000° F (1366 K) exposure (fig. 2(c)) showed a rather uniform white scale when viewed under polarized light. The scale was about 0.2 mil (5 μm) thick with no preferential grain boundary oxidation. Even after 600 hours at 2200° F (1478 K), this scale was only 1.4 mils (35 μm) thick. The high temperature, however, developed a pink scale similar to that observed for the 2000° F (1366 K) scales on GE 1541. The substrate grain size after exposure was very large, and a small amount of unidentified second phase can be seen uniformly distributed throughout the substrate.

XRD analysis (see table V(a)) on the 600-hour 2000° F (1366 K) specimen as well as on the 600-hour 1800° F (1478 K) specimen showed that the major scale phase was alpha Al_2O_3 (corundum). No crystalline silica was found on XRD even though the substrate contained about 1 percent silicon. The thicker scales formed at 2200° F (1478 K), however, contained alpha cristobalite (a form of SiO_2) and zirconia (ZrO_2).

Since no zirconium had been reported in the chemical analysis (table I), the presence of minor amounts of ZrO_2 was not expected. XRF analysis (table V(b)), however, indicated the presence of zirconium in the substrate and its growing concentration in the scale with increasing time and temperature. Although zircon crucibles were used in the oxidation exposure, no other alloys showed such high ZrO_2 concentrations on the surface.

The difference in the detection of SiO_2 at 2000° and 2200° F (1366 and 1478 K) can be attributed to the fact that silica films that develop at 2000° F (1366 K) and below are generally amorphous and are thus not detected as a discrete phase by XRD. Around 2200° F (1478 K), however, these amorphous films can revert to crystalline silica. The change in the color of the alumina scale may further indicate that the amorphous layer is serving as a diffusion barrier to some metal ions and preventing the contamination and coloration of the alumina scale. When amorphous SiO_2 no longer existed, chromium was detected by XRF in the pink scale scraped off the 2200° F (1478 K) specimen. It is well known that ruby is aluminum oxide with several percent chromium in solution.

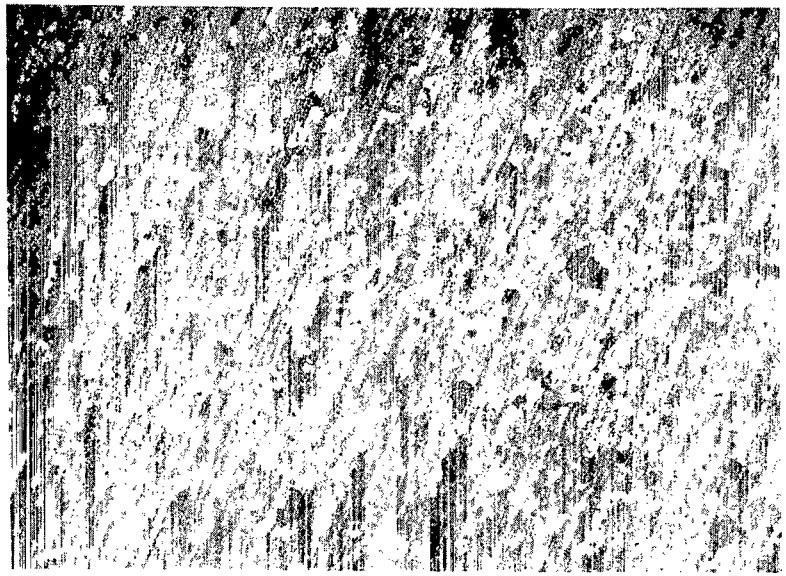

(a) After 4 hours at 1800° F (1254 K).

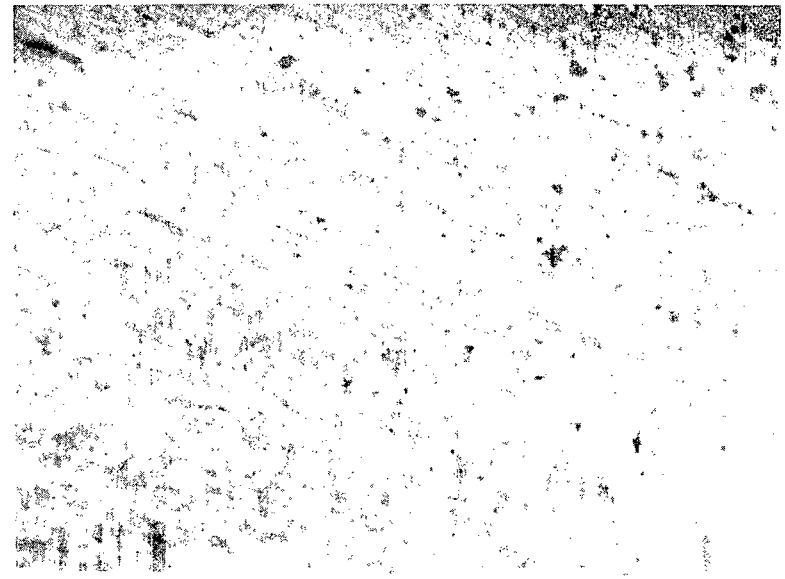

(b) After 600 hours at 1800° F (1254 K).

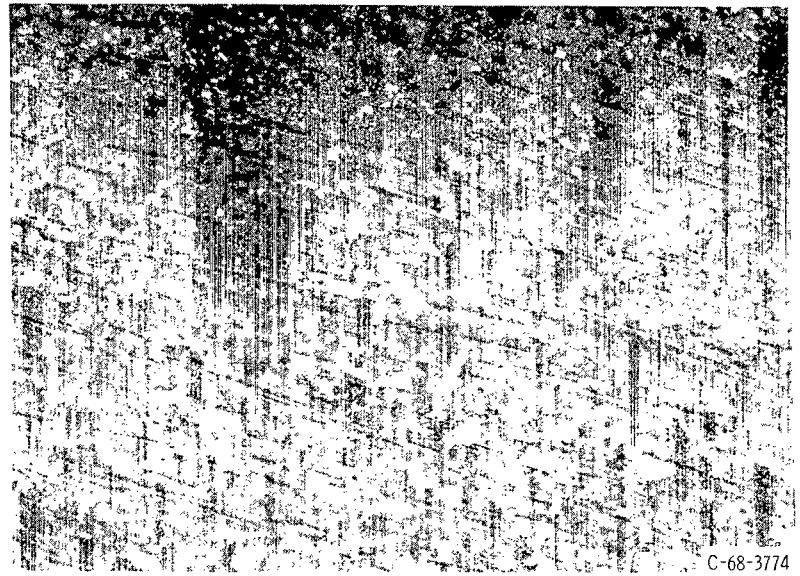

(c) After 4 hours at 2200° F (1478 K).

Figure 3. - Surface photographs of developing scale on HS-875. X50.

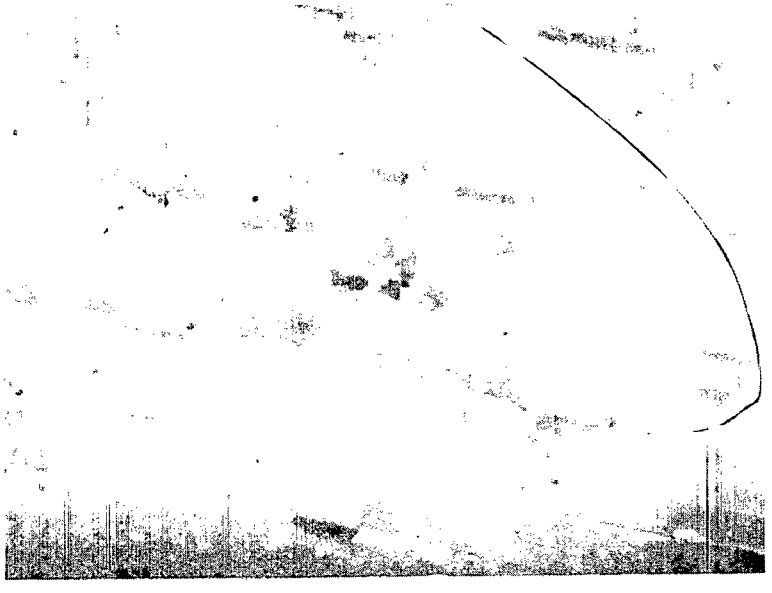

(d) After 100 hours at 2200° F (1478 K).

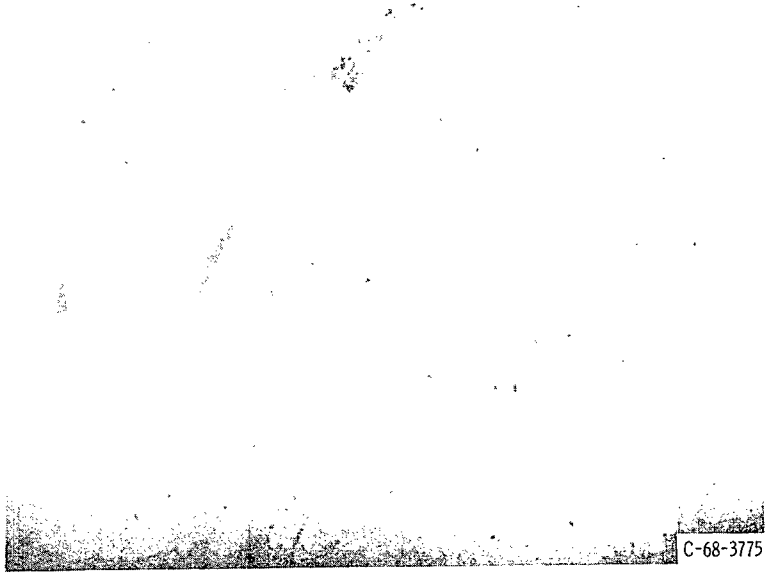

(e) After 600 hours at 2200° F (1478 K).

Figure 3. - Concluded.

The adherence of the scale on this alloy may well be related to the presence of SiO_2 or even ZrO_2 since the experiments of Hagel (ref. 6) involved similar Fe-25Cr-4Al alloys without silicon or zirconium. Under oxidation test, those alloys without silicon or zirconium showed widespread spalling of the alumina scale. Again, the spall analyses produced no meaningful information.

In general, the Fe-Cr-Al alloys are very oxidation resistant. It appears that this can be related to the presence of an Al_2O_3 scale which is known to be a good diffusion barrier for both metal and oxygen ions. Furthermore, both iron and chromium form oxides which are isomorphous with Al_2O_3 so some substitution of these for aluminum in the oxide lattice can occur without a disruptive influence on the scale.

NICKEL-BASE ALLOYS

Nickel and Nickel-Chromium Type

TD-Ni. - The simplest alloy in this series is TD-Ni which is very pure nickel containing a 2 volume percent dispersion of thorium dioxide (ThO_2). Table II shows that after a 600-hour exposure at 2000° F (1366 K), this material had gained over 31 milligrams per square centimeter and had a spall weight of 15 milligrams per square centimeter. The retained oxide scale was dark grey and was 11 mils (280 μm) thick.

A cross section of the metal-retained oxide scale is shown in figure 4(a). The massive oxide scale appears to be in two layers. The outer layer is columnar and contains large voids, while the inner layer appears to be equiaxed and contains many small voids. When viewed under polarized light, the inner layer appears bright green while the outer layer appears black - a situation typical of the scales formed on pure nickel. Under polarized light both nickel and chromium oxides appear green. Nickel oxide (NiO) is usually a lighter green than Cr_2O_3. Contrary to the internal oxidation found by Pettit and Felten (ref. 7) and the nonuniform attack and internal oxidation found by Wlodek (ref. 8), no internal oxidation or nonuniformity of attack was observed in this study. The substrate grains show orientation etching effects as evidenced by the apparent "stringer" slightly beneath the oxide-metal interface in figure 4(a).

XRD (table VI(a)) determined that the major phase present in both scale and spall was NiO with minor amounts of ThO_2. The lattice parameter of NiO was determined to be 4.177±0.004 Å in the scale and 4.176±0.004 Å in the spall. These findings agree with those of Wlodek (ref. 8) who found the outer layer to have an a_o of 4.177 Å. Wlodek further analyzed the inner layer and found its a_o to also be 4.177 Å. XRF (table VI(b)) found thorium (Th) in both the scale and the spall and also detected a small amount of chromium.

TD-NiCr. - TD-NiCr is a Ni-20Cr alloy dispersion strengthened with 2 volume percent of ThO_2. In contrast to TD-Ni, it has very good furnace oxidation resistance. After 600 hours at 2000° F (1366 K), this material gains only 0.8 milligram per square centimeter and has a spall weight of 0.7 milligram per square centimeter (table II). The scale thickness after such an exposure is only 0.2 mil (5 μm); and even after 600 hours at 2200° F (1478 K), it is only 0.7 mil (17.8 μm).

A cross section of this material after the 600-hour 2000° F (1366 K) exposure is shown in figure 4(b). The scale is very thin and under polarized light is dark green indicating Cr_2O_3. The substrate appears to contain very large grains within which appear partially agglomerated dispersoids. Furthermore, based on observations at various time-temperature conditions large voids develop in this material to a very great depth after oxidation exposure. The origin of the voids is not clear.

XRD (table VII(a)), supplemented by XRF (table VII(b)), verified the observation that the scale was Cr_2O_3. Furthermore, a small amount of ThO_2 was detected, but because of the very thin scale this may have been detected in the substrate. The amount of spall produced was very small. Meaningful data were not obtained on spall composition.

A large number of studies have been made on the oxidation behavior of nickel-chromium alloys. In most alloys of this type, a number of impurities are added to improve cyclic oxidation resistance. Some of these elements promote the formation of spinels. In the case of TD-NiCr containing only nickel and chromium, only the Cr_2O_3 was observed in the scale. Likewise, Gulbransen and Andrew (ref. 9) found a low silicon, low manganese alloy to form essentially Cr_2O_3 with only traces of a spinel of a_o of 8.33 Å - most likely $NiCr_2O_4$. Those investigators such as Ignatov and Shamgunova with less pure alloys (ref. 10) found more spinel on the surface and Cr_2O_3 only at the metal-scale interface showing spinel formation to be dependent on small percentages of impurities such as manganese.

Chromel A. - Chromel A is a Ni-20Cr alloy with additions of less than about 1 percent silicon or manganese. After 600 hours at 2000° F (1366 K), it showed a weight gain of 6.5 milligrams per square centimeter and a spall weight of 16.7 milligrams per square centimeter (see table II). The retained scale thickness after the aforementioned exposure is about 1.3 mils (32 μm) with some oxide fingers penetrating down to 6 mils (152 μm).

In cross section, very little scale has been preserved, as shown in figure 4(c). Under polarized light, the scale was green indicating Cr_2O_3 and was dotted with a black phase - probably spinel. At the substrate-scale interface, grey areas of an unknown composition were also observed. In the substrate, as judged by a number of time-temperature conditions, considerable porosity developed beneath the scale and the typical twinned structure of nickel-chromium alloys was observed. This is in contrast to TD-

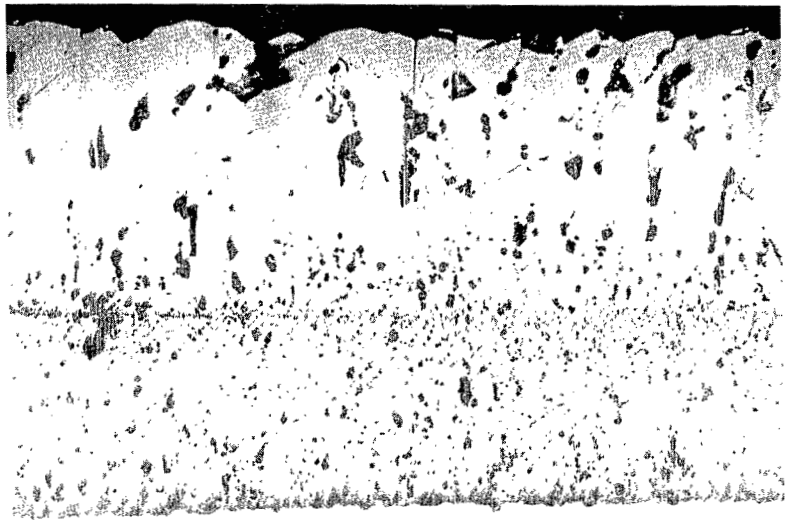

(a) TD-Ni. X250.

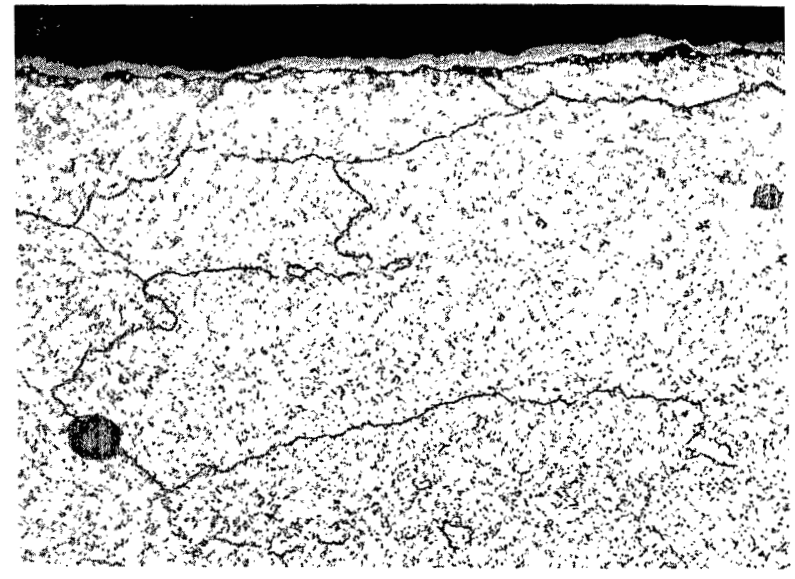

(b) TD-NiCr.

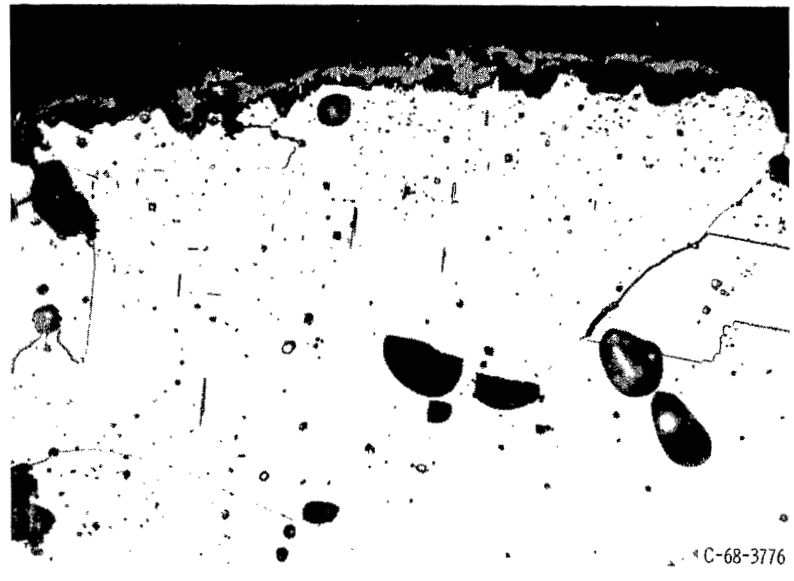

(c) Chromel A.

Figure 4. - TD-nickel and nickel-chromium type alloys after 600 hours in air at 2000° F (1366 K). X500 (unless otherwise noted).

NiCr which showed no twinning. Furthermore, the grain size of this substrate was quite large.

XRD data (table VIII(a)) indicated Cr_2O_3 to be the major retained scale phase with minor amounts of spinel present. The lattice constant of the spinel was 8.33±0.02 Å which is a good match for the expected $NiCr_2O_4$.

The spall also contained Cr_2O_3 and more spinel than in the scale. The spinel contained predominantly nickel and chromium (table VIII(b)).

The dominance of Cr_2O_3 in the scale again indicate the preference for this phase on oxidized Ni-20Cr alloys that contain only minor additions.

DH242. - DH242 is similar to Chromel A but contains about 1 percent of niobium (Nb), tantalum (Ta), and iron. This alloy gained about 5.9 milligrams per square centimeter after 600 hours at 2000° F (1366 K) and had a spall weight of 9.7 milligrams per square centimeter as shown in table II. After the aforementioned exposure, the scale thickness was about 1.1 mils (27 μm), similar to Chromel A. However, the finger-like oxide projections extended deeper into the substrate with DH242, while the amount of void formation was somewhat less with this alloy (fig. 4(d)) than was observed with Chromel A, as shown in figure 4(c). When viewed under polarized light, this retained scale was essentially the same as that of Chromel A - the major phase was green indicating Cr_2O_3 and a dark phase - spinel - was dispersed in it.

XRD (table IX(a)) confirms the presence of Cr_2O_3 in the scale but detects no spinel until after 600 hours at 2200° F (1478 K). XRF (table IX(b)) also shows chromium concentrating in the scale and finds nickel as well. There is also a slight concentration of niobium in the scale but no oxides of niobium were detected.

The spall shows the presence of both Cr_2O_3 and a spinel with a_o of 8.38±0.02 Å. This lattice constant is above that of pure $NiCr_2O_4$, and along with the concentration of iron in the spall detected by XRF, indicates that the spinel lattice has been enlarged in accordance with the trend shown in figure 1. The spinel may be of the $(Ni, Fe)Cr_2O_4$ composition.

The data collected on specimens exposed at 2200° F (1478 K) for up to 600 hours show that the relative amount of chromium is decreasing in the scale with time. This indicates that at such high temperatures, chromium is being lost via vaporization or that more spinel is being formed that contains lower chromium.

Bendel. - Bendel is similar to some of the previously mentioned Ni-20Cr alloys in that it contains small amounts of both silicon and manganese. It differs in two major aspects: first, it contains 35 weight percent chromium and, secondly, it has 3 weight percent dispersion of $MgAl_2O_4$. This alloy gained 8.8 milligrams per square centimeter after 600 hours at 2000° F (1366 K) and spalled more than any other simple nickel alloy (i.e., 20.2 mg/cm^2 - even more than TD-Ni as shown in table II). The depth of penetration seemed to be around 4 mils (102 μm) maximum and was thus somewhat less than

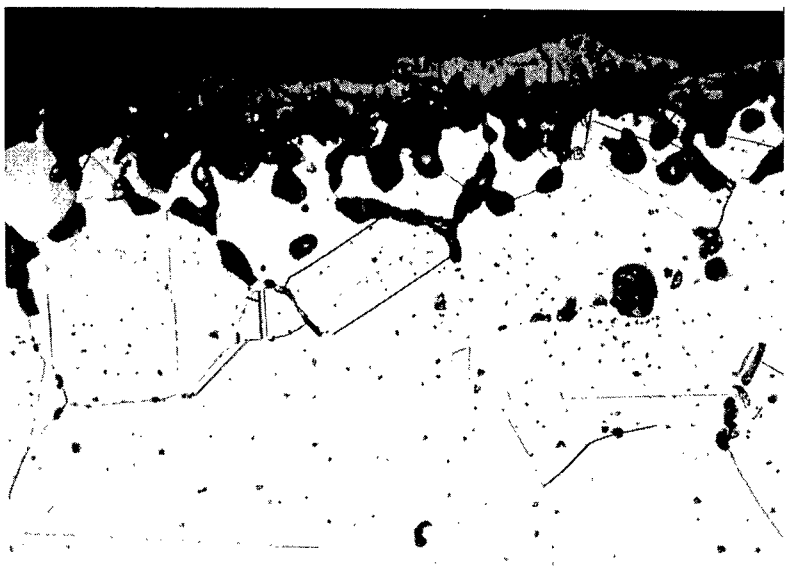

(d) DH242.

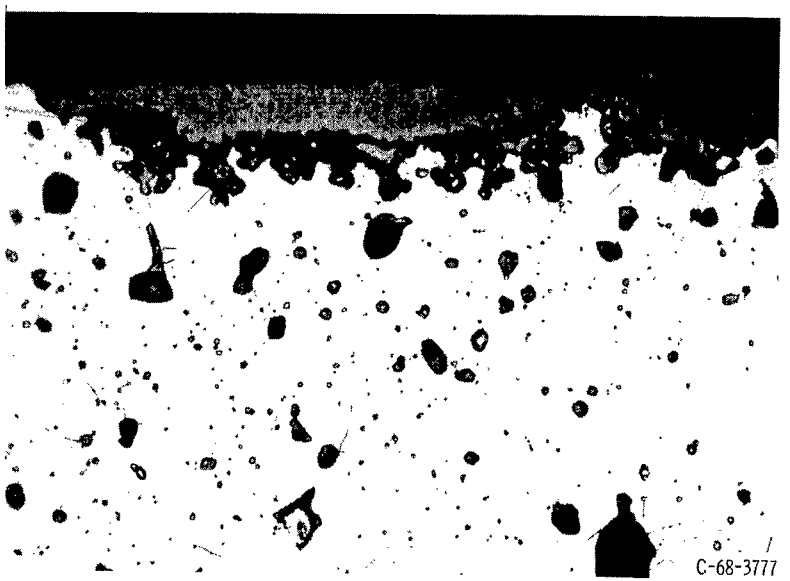

(e) Bendel.

Figure 4. - Concluded.

that of DH242. This can be seen in the microstructure shown in figure 4(e). The scale appears to grow inward at different rates in different areas as evidenced by the dished out areas. Under polarized light, this scale is dark green near the surface and becomes lighter green near the substrate interface.

The aluminate spinel particles are quite large. These particles seem to have limited the amount of grain growth in the substrate during exposure. Also, the twinned structure appears to be more evident in this alloy than in others after the same thermal exposure.

XRD (table X(a)) found the scale to be primarily Cr_2O_3. The spall contained both Cr_2O_3 and a spinel of $a_o = 8.35 \pm 0.02$ Å - again somewhat high for pure $NiCr_2O_4$. XRF (table X(b)) showed that both manganese and iron are concentrated in the spall with a very high chromium intensity being detected. Again, the presence of manganese and iron is reflected in the higher lattice parameter of the spinel which may be of the $(Ni, Mn)(Cr, Fe)_2O_4$ type. No iron was noted in the chemical analysis of this material (table I), however.

Complex Nickel-Base Alloys

Hastelloy X. - Hastelloy X is reputed to be one of the most oxidation resistant of the commercial complex nickel-base alloys. After the 600-hour 2000° F (1366 K) exposure, this alloy gained only 4.3 milligrams per square centimeter and spalled only 6.4 milligrams per square centimeter (table II). This is much better than the simpler nickel-chromium type alloys. Further, the retained oxide scale was 1.4 mil (35 μm) thick and maximum depth of penetration was about 5 mils (132 μm) after the aforementioned exposure.

Figure 5 shows the typical progression of complete alloy scale development. After 4 hours at 1800° F (1254 K), a temperature chosen so as to extend the time between gross changes, dark spots can be seen to be developing along surface scratches (see fig. 5(a)). These are Cr_2O_3. When 100 hours have passed (fig. 5(b)), almost the entire surface is overgrown with the dark phase and some lighter phase can be seen to be forming. After 600 hours (fig. 5(c)), both light and dark regions are apparent indicating an intermixing of several oxide phases.

In cross section, the 600-hour 2000° F (1366 K) specimen (see fig. 6(a)) shows a tightly adherent scale with large voids below the surface extending to a depth of about 10 mils (254 μm). The scale is green under polarized light. It is light green near the substrate, while it gradually darkens near the surface. This indicates either a change in the Cr_2O_3 or the presence of a finely dispersed, dark second phase. The carbide phase in the substrate agglomerates after long-time exposure but is not visible in figure 6(a) since the region near the surface has been depleted of carbides.

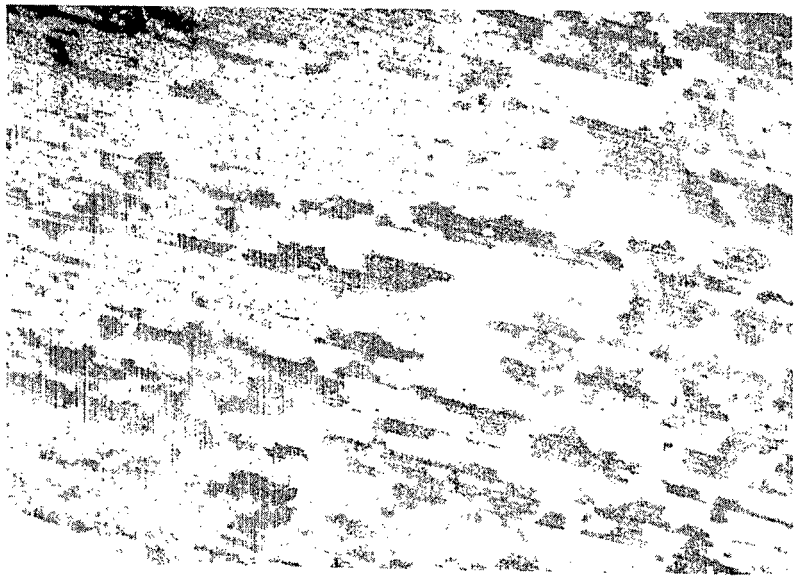

(a) After 4 hours.

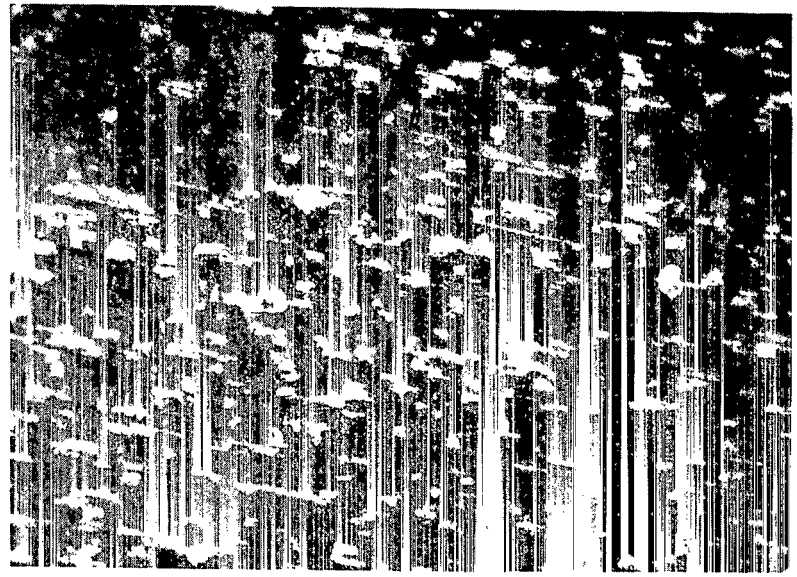

(b) After 100 hours.

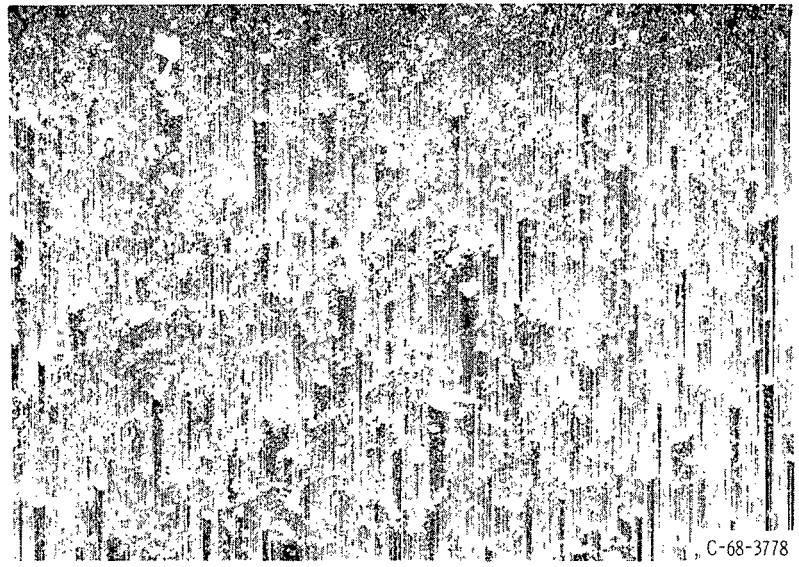

(c) After 600 hours.

Figure 5. - Surface photographs of developing scale on Hastelloy X at 1800° F (1254 K). X50.

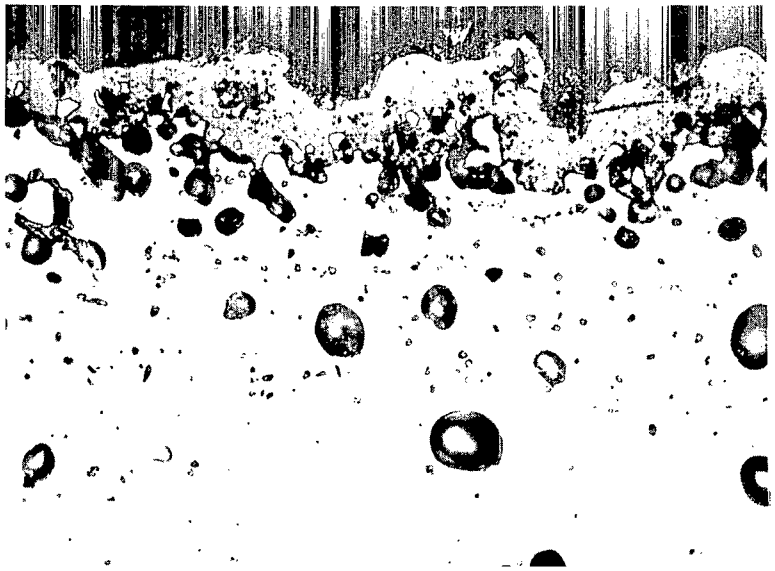

(a) Hastelloy X.

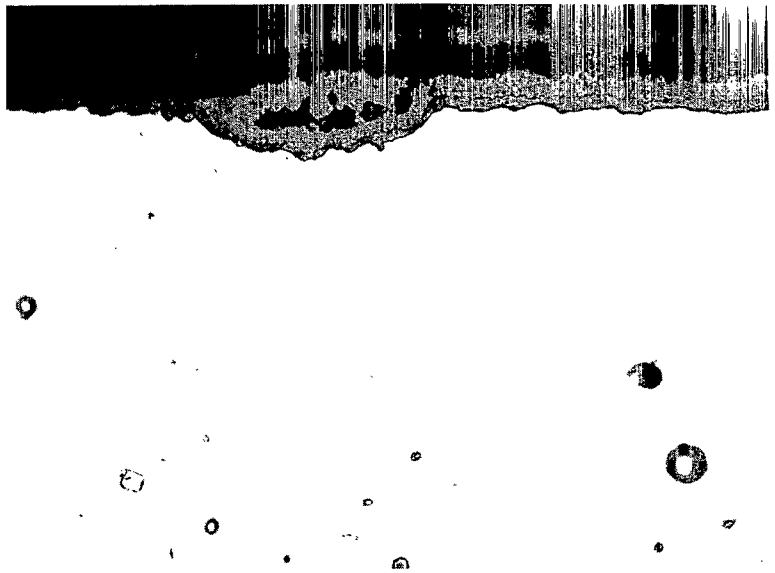

(b) Udimet 500.

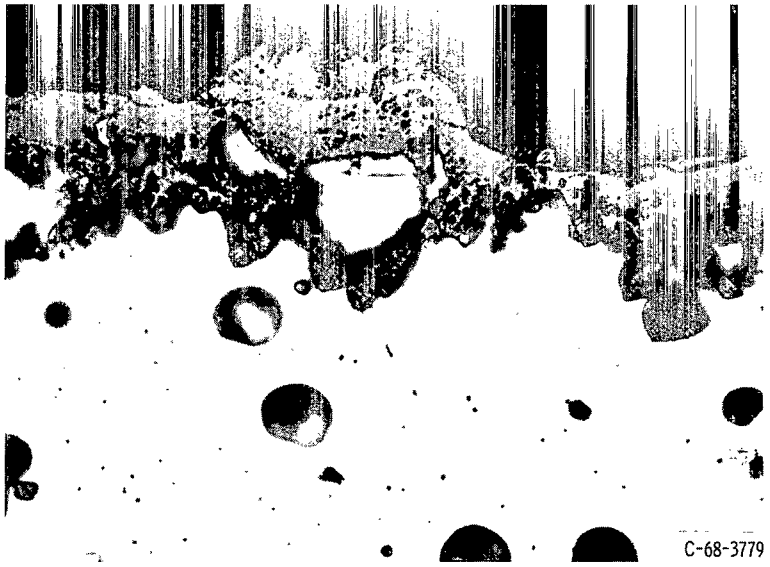

(c) RA 333.

Figure 6. - Complex nickel-base alloys after 600 hours in air at 2000° F (1366 K). X500.

XRD (table XI(a)) shows that scales at both 1800° and 2000° F (1254 and 1366 K) to contain major fractions of both Cr_2O_3 and a high lattice parameter spinel of a_o = 8.37±0.02 to 8.39±0.02 Å. The spall at 2000° F (1366 K) is similar to the scale. After 600 hours at 2200° F (1478 K), the major phase in the retained scale is Cr_2O_3 and the spinel is no doubt heavily concentrated in the spall. XRF (table XI(b)) shows that chromium and manganese concentrate in both the scale and the spall. Thus, the spinel no doubt contains significant manganese which raises the value of the lattice parameter as shown in figure 1. The spinel is probably an $(Fe, Ni)(Cr, Mn)_2O_4$ type.

Molybdenum (Mo) also concentrates in the retained scale at both 1800°, 2000°, and 2200° F (1254, 1366, and 1478 K) (see table XI(b)), but no molybdenum compounds were found by XRD. Since no molybdenum was detected in the spall by XRF, molybdenum probably has been lost via vaporization of MoO_3.

There have been several studies on the oxidation behavior of Hastelloy X (refs. 11 and 12 among others). The results of this study differ from those of a study made by Wlodek (ref. 12). He found that on cooldown the oxides spalled cleanly from the metal. This study found retained scale. The difference may be that Wlodek conducted noncyclic tests on electropolished specimens and that the stresses developed in the thick scale were so great as to cause shear at the interface.

Wlodek found a higher lattice parameter spinel (a_o = 8.4 to 8.5 Å) than reported herein. He also found that amorphous silica existed at the metal-scale interface. In the studies described in this report, no evidence of SiO_2 was detected even after the 2200° F (1478 K) exposures where silica would be expected to become crystalline.

Udimet 500. - This alloy retained about the same weight of scale as Hastelloy X (i.e., 4.2 mg/cm^2) after 600 hours at 2000° F (1366 K), but the amount of spall was considerably more (16.9 mg/cm^2 (table II)). However, the scale thickness was only about 1.5 mils (37 μm), and there was very little oxide penetration (see fig. 6(b)). Under polarized light, the inner layer of the retained scale appeared light blue.

The outer scale layer was dark blue. This indicates that the scale was probably $CoAl_2O_4$. Some dark islands were scattered in this scale - probably a spinel. The substrate itself showed very shallow depletion and relatively few voids below the scale interface. Some twinning and moderate grain growth were observed, but these are not visible in the lightly etched microstructure shown in figure 6(b).

XRD (table XII(a)) confirmed the presence of (Ni,Co)O in the retained scale. Also in the scale was considerable spinel with a very low lattice parameter a_o of 8.10±0.02 Å. The scale was studied by XRF (table XII(b)). Little chromium was found and essentially only nickel and cobalt were detected. A small amount of titanium was also found in the scale but no titanium compounds were detected by XRD. Since aluminum cannot be detected by standard XRF, the scale spinel is believed to be either $NiCo_2O_4$ (see fig. 1), $(Ni, Co)Al_2O_4$ whose lattice parameter is 8.046±0.02 Å, or a mixture of both. The spall

from this alloy is different from the retained scale in that both Cr_2O_3 (minor phase) and an 8.31±0.02 Å spinel (major phase) were found. From figure 1, the spall was probably a (Ni, Co)Cr_2O_4 spinel.

RA 333. - This alloy is very high in both iron and chromium and showed both the highest weight gain (8.0 mg/cm^2) and the greatest spall weight (20.2 mg/cm^2) of any of the complex nickel alloys after 600 hours at 2000^o F (1366 K) (table II). The retained scale thickness was 1.5 mils (37 μm).

The microstructure of the scale-substrate cross section is shown in figure 6(c). The scale is irregular with patches of a second phase being retained on the surface. Polarized light showed a green Cr_2O_3 scale gradually darkening away from the metal interface with dark patches of the second phase on the surface. Brown islands of spinel were also observed. Extensive void formation and localized oxide penetration to a depth of 7 mils (178 μm) were noted. A depleted zone (not completely shown) extended several mils beyond the depth of oxide penetration.

XRD (table XIII(a)) detected Cr_2O_3 and spinel in both scale and spall, with more Cr_2O_3 in the retained scale than in the spall. XRF (table XIII(b)) shows some concentration of chromium and manganese in the retained scale indicating that the spinel, whose a_o is 8.44±0.02 Å, is probably Ni(Cr, Mn)$_2O_4$. In the spall, XRF shows the concentration of chromium, manganese, and iron. The spinel in the spall has an a_o of 8.40±0.02 Å; and by using the data of figure 1, it may be more closely described as (Ni, Fe)(Cr, Mn)$_2O_4$.

COBALT-BASE ALLOY

L-605

L-605 was the only cobalt-base alloy included in the oxidation studies. It contains 20 weight percent chromium, 10 weight percent nickel, and 16 weight percent tungsten as the major alloying elements. After a 600-hour exposure at 2000^o F (1366 K), this alloy gained 36.1 milligrams per square centimeter - more than any other alloy other than N-155. Further, the spall weight was 112 milligrams per square centimeter - again more than any other alloy other than N-155 (table II). In general, the retained scale was rather uniform in thickness; but after long-time exposures at both 1800^o and 2000^o F (1254 and 1366 K), some fingers of oxide developed which penetrated the substrate as shown in figure 7. After 600 hours at 2000^o F (1366 K) the scale (1.5 mils or 37 μm thick) can be seen to consist of several layers. Under polarized light, green Cr_2O_3, blue $CoAl_2O_4$, and several dark phases could be detected in the scale. Beneath the scale, the Co_2W Laves phase is depleted to a depth of greater than 4 mils (102 μm). Furthermore, voids can be detected in the depleted zone, although the total number and volume of voids are not as great as were observed in some of the previous alloys.

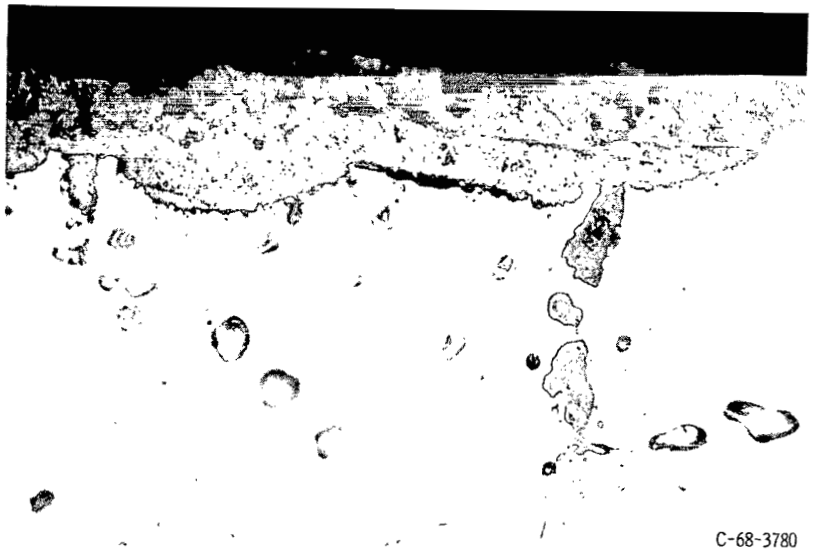

Figure 7. - Cobalt-based alloy L-605 after 600 hours in air at 2000° F (1366 K). X500.

With increasing time at 1800° F (1265 K) and even at 4 hours at 2000° F (1366 K), phases besides the predominant (Co, Ni)O were detected (see table XIV). The lattice parameter of the spinel appeared to become larger with both increasing time and temperature. It ranged from 8.20±0.02 to 8.29±0.02 Å over the span of 4 hours at 1800° F (1254 K) to 600 hours at 2000° F (1366 K). By using XRF and figure 1 data, the spinel is probably (Co, Ni)Cr_2O_4. Spinel became the single major phase after 100 hours at 2000° F (1366 K). Other phases detected were (Co, Ni)O, $CoWO_4$, and Cr_2O_3. The spall after 600 hours at 2000° F (1366 K) was predominantly $CoWO_4$ and (Co, Ni)O.

SUMMARIZING REMARKS AND CONCLUSIONS

Selected samples of 12 commercial heat resisting alloys were studied after cyclic furnace oxidation tests at temperatures of from 1400° to 2200° F (1033 to 1478 K). Consecutive cycles at 4, 16, 64, 100, 200, 300, 400, 500, and 600 hours of exposure were used to develop surface oxide scales and spall over a wide range of time. The majority of the metallography, X-ray fluorescence, and X-ray diffraction studies on both the in situ scales and spall were conducted on samples that had been exposed for 600 hours at 2000° F (1366 K).

The following table summarizes the weight change and spall data as well as the scale composition and characterization information for specimens exposed at 2000° F (1366 K) for 600 hours. (The alloys are listed in order of decreasing oxidation resistance under the cyclic furnace conditions used in this study.):

Alloy (base element)	Weight gain, mg/cm^2 (a)	Total spall, mg/cm^2 (a)	Major (and minor) scale constituents (b)	Major (and minor) spall constituents (b)
TD-NiCr (Ni)	0.8	~0.7	Cr_2O_3; (ThO_2)	Light spall - composition did not correlate with alloy chemistry
HS-875 (Fe)	0.9	~0.5	αAl_2O_3	Light spall - composition did not correlate with alloy chemistry
GE 1541 (Fe)	1.1	~0.4	αAl_2O_3	Light spall - composition did not correlate with alloy chemistry
Hastelloy X (Ni)	4.3	6.4	Cr_2O_3, $(Fe, Ni)(Cr, Mn)_2O_4$ $a_o = 8.39 \pm 0.02$ Å	Cr_2O_3, $(Fe, Ni)(Cr, Mn)_2O_4$ $a_o = 8.39 \pm 0.02$ Å
Udimet 500 (Ni)	4.2	16.9	$(Ni, Co)O$, $(Ni, Co)(Co, Al)_2O_4$ $a_o = 8.10 \pm 0.02$ Å	$(Ni, Co)Cr_2O_4$, $a_o = 8.31 \pm 0.02$ Å; (Cr_2O_3)
DH242 (Ni)	5.9	9.7	Cr_2O_3	Cr_2O_3, $(Ni, Fe)\ Cr_2O_4$ $a_o = 8.38 \pm 0.02$ Å
Chromel A (Ni)	6.5	16.7	Cr_2O_3; ($NiCr_2O_4$ $a_o = 8.34 \pm 0.02$ Å)	Cr_2O_3, $NiCr_2O_4$ $a_o = 8.33 \pm 0.02$ Å
RA 333 (Ni)	8.0	20.2	Cr_2O_3, $Ni(Cr, Mn)_2O_4$ $a_o = 8.44 \pm 0.02$ Å	Cr_2O_3, $(Ni, Fe)(Cr, Mn)_2O_4$ $a_o = 8.40 \pm 0.02$ Å
Bendel (Ni)	8.8	20.2	Cr_2O_3	Cr_2O_3, $(Ni, Mn)(Cr, Fe)_2O_4$ $a_o = 8.35 \pm 0.02$ Å
TD-Ni (Ni)	31.1	15.0	NiO; (ThO_2)	NiO; (ThO_2)
L-605 (Co)	36.1	112.0	$(Ni, Co)(Co, Cr)_2O_4$, $a_o = 8.29 \pm 0.02$ Å; ((Co, Ni)O)	$CoWO_4$, (Co, Ni)O
N-155 (Fe)	45.0	250.0	Cr_2O_3, $(Ni, Co)(Cr, Fe)_2O_4$ $a_o = 8.32 \pm 0.02$ Å	γFe_2O_3, $(Ni, Co)(Cr, Fe)_2O_4$ $a_o = 8.34 \pm 0.02$ Å

[a]Data from NASA CR-930.
[b]a_o = lattice parameter in Å (or $\times 10^{-10}$ m).

The most oxidation resistant alloys were TD-NiCr and the two Fe-Cr-Al type alloys, HS-875, and GE 1541. Each of these alloys formed only a single oxide of the M_2O_3 type. This type scale appears to best inhibit further oxidation of the substrate and also tends to spall very little.

The remaining nickel-base alloys formed spinels such that spinel was detected in all of the spalls and in every retained scale but that on Bendel. These alloys also generally formed a second major scale and spall phase with the exception of TD-Ni, the latter forming only NiO, a recognized poor oxygen and nickel ion diffusion barrier. The spalling connected with such two-phase scales suggests that the presence of a mixed oxide scale promotes spalling. There is no apparent correlation between oxidation degradation

as expressed by weight gain and spall weight and between spinel composition or lattice parameter.

The remaining iron alloy, N-155, showed a two-phase scale and poor oxidation and spall resistance.

The L-605 cobalt alloy apparently suffers from a severe spalling problem.

Lewis Research Center,
National Aeronautics and Space Administration,
Cleveland, Ohio, October 16, 1968,
129-03-05-03-22.

REFERENCES

1. Cole, Fred W.; Padden, James B.; and Spencer, Andrew R.: Oxidation Resistant Materials for Transpiration Cooled Gas Turbine Blades. Part I: Sheet Specimen Screening Tests. NASA CR-930, 1968.

2. Verwey, E. J. W.; and Heilmann, E. L.: Physical Properties and Cation Arrangement of Oxides With Spinel Structures. I. Cation Arrangements in Spinels. J. Chem. Phys., vol. 15, no. 4, Apr. 1947, pp. 174-180.

3. Verwey, E. J.; Haayman, P. W.; and Romeijn, F. C.: Physical Properties and Cation Arrangement of Oxides with Spinel Structures. II. Electronic Conductivity. J. Chem. Phys., vol. 15, no. 4, Apr. 1947, pp. 181-187.

4. Anon.: 16th Set of Inorganic Powder Diffraction File. ASTM, 1966.

5. Anon.: Fifth Annual Report - High Temperature Materials Programs, Part A. Rep. GEMP-400A, General Electric Co., Feb. 28, 1966.

6. Hagel, W. C.: The Oxidation of Iron, Nickel and Cobalt-Base Alloys Containing Aluminum. Corrosion, vol. 21, no. 10, Oct. 1965, pp. 316-326.

7. Pettit, Fredrick S.; and Felton, Edward J.: The Oxidation of Ni-2ThO_2 between 900° and 1400° C. J. Electrochem. Soc., vol. 111, no. 2, Feb. 1964, pp. 135-139.

8. Wlodek, S. T.: The Oxidation of Ni-2% ThO_2. Rep. R62FPD140, General Electric Co., May 4, 1962.

9. Gulbransen, Earl A.; and Andrew, Kenneth F.: Oxidation Studies on the Nickel-Chromium and Nickel-Chromium-Aluminum Heater Alloys. J. Electrochem. Soc., vol. 106, no. 11, Nov. 1959, pp. 941-948.

10. Ignatov, D. V.; and Shamgunova, R. D.: Mechanism of the Oxidation of Nickel and Chromium Alloys. NASA TT F-59, 1961.

11. Baciarelli, R. M.: Army Gas-Cooled Reactor Systems Program. Isothermal Oxidation of Hastelloy X at 1750^{o} and 1850^{o} F in Air. Rep. AGN-TM-413, Aerojet-General Nucleonics, Dec. 1965.

12. Wlodek, S. T.: The Oxidation of Hastelloy Alloy X. Trans. AIME., vol. 230, no. 1, Feb. 1964, pp. 177-185.

TABLE I. - ALLOY CHEMICAL ANALYSES (REF. 1)

[Weight percent except when indicated otherwise.]

Alloy	Analysis[a]	Carbon	Manganese	Silicon	Chromium	Nickel	Cobalt	Molybdenum	Tungsten	Niobium and tantalum	Titanium	Aluminum	Iron	Copper	Sulfur	Phosphorus	Other
N-155[b]	V	0.10	1.51	0.73	21.35	20.26	19.93	2.98	2.50	1.02	------	----	Balance	------	0.011	0.020	---------
	I	0.10	1.76	0.80	21.51	20.16	19.93	2.64	2.25	1.20	------	----	Balance	------	0.012	0.007	---------
GE 1541[c]	V	------	----	28 ppm	15.36	-----	-----	----	-----	----	------	4.19	Balance	35 ppm	17 ppm	70 ppm	0.43 Y
	I	0.01	0.02	0.03	13.64	-----	-----	----	-----	----	------	4.20	Balance	------	0.003	0.004	0.88 Y
HS-875[d]	V	------	----	------	22.35	-----	-----	----	-----	----	------	5.80	Balance	------	------	-----	---------
	I	0.03	0.25	0.91	22.25	-----	-----	----	-----	----	------	5.39	Balance	------	0.005	0.005	---------
TD-Ni[e]	V	0.0009	----	------	<0.01	Balance	<0.01	----	-----	----	<0.001	----	<0.01	<0.001	0.001	-----	2.6 ThO_2
	I	0.02	----	------	-----	98.64	-----	----	-----	----	------	----	-------	------	0.002	0.006	---------
TD-NiCr[e]	V	62 ppm	----	------	20.72	Balance	-----	----	-----	----	------	----	-------	------	18 ppm	-----	2.6 ThO_2
	I	0.01	----	------	20.61	Balance	-----	----	-----	----	------	----	-------	------	0.029	0.012	---------
Chromel A[d]	V	------	0.20	1.40	20.0	78.0	-----	----	-----	----	------	----	-------	------	------	-----	---------
	I	0.02	0.05	0.74	20.61	78.6	-----	----	-----	----	------	----	-------	------	0.006	0.004	---------
DH242[f]	V	0.02	0.08	0.96	19.4	Balance	-----	----	-----	1.28	------	----	0.96	------	------	-----	---------
	I	0.04	0.02	1.16	22.28	Balance	-----	----	-----	1.03	------	----	1.40	------	0.005	0.005	---------
Bendel[g]	V	------	----	------	34.0	63.0	-----	----	-----	----	------	----	-------	------	------	-----	3.0 spinel
	I	0.09	0.13	0.81	35.89	61.90	-----	----	-----	----	------	----	-------	------	0.007	0.011	---------
Hastelloy X[b]	V	0.015	0.57	0.84	22.47	Balance	0.93	9.12	0.57	----	------	----	18.35	------	0.007	0.018	---------
	I	0.03	0.57	0.78	21.54	Balance	1.64	8.52	0.73	----	------	----	19.81	------	0.006	0.006	---------
Udimet 500[h]	V	0.07	<0.1	<0.1	18.9	Balance	19.1	4.05	-----	----	3.01	3.00	0.18	<0.1	0.003	-----	---------
	I	0.07	0.05	0.04	19.06	Balance	19.40	4.30	-----	----	3.05	3.17	0.01	------	0.005	0.003	---------
RA 333[i]	V	0.03	1.34	0.94	25.80	46.87	2.81	2.80	2.93	----	------	----	Balance	0.03	0.008	0.012	---------
	I	0.07	1.20	0.82	24.89	46.08	3.05	2.60	3.72	----	------	----	Balance	------	0.023	0.011	---------
L-605[b]	V	0.11	1.45	0.16	19.81	10.04	Balance	----	14.61	----	------	----	1.80	------	0.008	0.023	---------
	I	0.10	1.25	0.18	19.89	10.32	Balance	----	15.78	----	------	----	2.03	------	0.015	0.004	---------

[a] V = vendor's analysis.
I = independent laboratory analysis.
[b] Union Carbide Corp.
[c] General Electric Co.
[d] Hoskins Manufacturing Co.
[e] E. I. duPont de Nemours & Co.
[f] Driver-Harris Co.
[g] Bendix Corp.
[h] Special Metals Corp.
[i] Rolled Alloys, Inc.

TABLE II. - CYCLIC FURNACE AIR

WEIGHT GAIN AND SPALL WEIGHT

AFTER 600 HOURS AT 2000° F

(1366 K) (REF. 1)

Alloy	Weight gain, mg/cm^2	Total spall, mg/cm^2
	Iron base	
N-155	45.0	250.0
GE 1541	1.1	~.4
HS-875	.9	~.5
	Nickel base	
TD-Ni	31.1	15.0
TD-NiCr	.8	~.7
Chromel A	6.5	16.7
DH242	5.9	9.7
Bendel	8.8	20.2
Hastelloy X	4.3	6.4
Udimet 500	4.2	16.9
RA 333	8.0	20.2
	Cobalt base	
L-605	36.1	112.0

TABLE III. - XRD AND XRF DATA ON N-155

(a) XRD data

Exposure temperature		Exposure time, hr	Sample location	Major phases	Minor phases	Trace
°F	K			(a)		
2000	1366	600	Scraped scale	Cr_2O_3, spinel a_o = 8.32±0.02 Å	----------	-----
			Spall	γFe_2O_3, spinel a_o = 8.34±0.02 Å	----------	-----

(b) XRF data

Exposure temperature		Exposure time, hr	Sample location	Element characteristic radiation intensity								
°F	K			(b)	CrKα	MnKα	FeKα	CoKα	NiKα	WLα	NbKα	MoKα
1400	1033	4	No scale	I	45.0	4.5	139.0	128.0	125.0	4.5	2.0	5.5
				R	0.188	0.032	1.000	0.921	0.899	0.032	0.014	0.039
2000	1366	600	In situ	I	103.0	1.00	30.0	45.0	77.0	8.5	3.4	8.0
				R	3.433	0.033	1.000	1.500	2.566	0.283	0.113	0.266
			Spall	I	45.3	7.8	97.6	105.5	93.2	3.0	1.6	1.6
				R	0.445	0.080	1.000	1.075	0.954	0.031	0.016	0.016

[a] a_o = lattice parameter in Å (or $\times 10^{-10}$ m).

[b] I = intensity = $\times 10^{-3}$ count/min of element.

R = intensity ratio = $I/I_{alloy\ base}$

TABLE IV. - XRD AND XRF DATA ON GE 1541

(a) XRD data

Exposure temperature		Exposure time, hr	Sample location	Major phases	Minor phases	Trace
°F	K			(a)		
1800	1254	600	Scraped scale	αAl_2O_3, Cr_2O_3	----------	-----
2000	1366	4	Scraped scale	αAl_2O_3	----------	-----
		100	Scraped scale	αAl_2O_3	----------	-----
		600	Scraped scale	αAl_2O3	----------	-----
			Spall[b]	Cr_2O_3, spinel $a_o = 8.34 \pm 0.02$	----------	-----

(b) XRF data

Exposure temperature		Exposure time, hr	Sample location	(c)	Element characteristic radiation intensity						
°F	K				CrKα	MnKα	FeKα	CoKα	NiKα	YKα	ZrKα
1400	1033	4	No scale	I	50.0	-----	419.0	-----	-------	3.1	-----
				R	0.119	-----	1.000	-----	-------	0.007	-----
1800	1254	4	In situ	I	45.0	-----	382.0	-----	-------	2.8	-----
				R	0.118	-----	1.000	-----	-------	0.007	-----
		100	In situ	I	33.0	-----	304.0	-----	-------	1.9	-----
				R	0.108	-----	1.000	-----	-------	0.006	-----
		600	In situ	I	38.5	-----	350.0	-----	-------	3.0	-----
				R	0.110	-----	1.000	-----	-------	0.009	-----
2000	1366	4	In situ	I	43.0	-----	368.0	-----	-------	2.7	-----
				R	0.117	-----	1.000	-----	-------	0.007	-----
		100	In situ	I	41.0	-----	375.0	-----	-------	3.3	-----
				R	0.109	-----	1.000	-----	-------	0.009	-----
		600	In situ	I	42.0	-----	350.0	-----	-------	3.6	-----
				R	0.120	-----	1.000	-----	-------	0.010	-----
			Spall[b]	I	31.7	9.0	35.5	0.6	27.5	-----	0.5
				R	0.893	0.253	1.000	0.017	0.775	-----	0.014

[a] a_o = lattice parameter in Å (or $\times 10^{-10}$ m).

[b] Results do not correlate with other compositional information on alloy.

[c] I = intensity = $\times 10^{-3}$ count/min of element.

R = intensity ratio = $I/I_{alloy\ base}$.

TABLE V. - XRD AND XRF DATA ON HS-875

(a) XRD data

Exposure temperature		Exposure time, hr	Sample location	Major phases	Minor phases	Trace
°F	K			(a)		
1800	1254	100	Scraped scale	αAl_2O_3	----------	-----
		600	Scraped scale	αAl_2O_3	----------	-----
2000	1366	600	Scraped scale	αAl_2O_3	----------	-----
			Spall[b]	Cr_2O_3, spinel a_o = 8.35±0.02 Å	----------	-----
2200	1478	4	Scraped scale	αAl_2O_3	αSiO_2	-----
		100	Scraped scale	αAl_2O_3	ZrO_2(t), ZrO_2(m)[c]	-----
		600	Scraped scale	αAl_2O_3	ZrO_2(t), ZrO_2(m)[c]	-----

(b) XRF data

Exposure temperature		Exposure time, hr	Sample location	Element characteristic radiation intensity						
				(d)	CrKα	MnKα	FeKα	CoKα	NiKα	ZrKα
°F	K									
1400	1033	4	No scale	I	69.0	1.0	345.0	-----	2.2	1.4
				R	0.200	0.003	1.000	-----	0.006	0.004
1800	1254	4	In situ	I	60.0	1.0	280.0	-----	1.7	1.2
				R	0.214	0.004	1.000	-----	0.006	0.004
		100	In situ	I	53.5	------	277.0	-----	2.0	1.0
				R	0.193	------	1.000	-----	0.007	0.004
		600	In situ	I	50.5	------	261.0	-----	2.0	1.4
				R	0.193	------	1.000	-----	0.008	0.005
2000	1366	600	In situ	I	49.0	1.0	253.0	-----	4.8	1.5
				R	0.194	0.004	1.000	-----	0.019	0.006
			Spall[b]	I	45.4	10.9	45.7	0.9	35.6	0.5
				R	0.993	0.238	1.000	0.020	0.779	0.011
2200	1478	4	In situ	I	55.0	------	282.0	-----	1.9	1.2
				R	0.195	------	1.000	-----	0.007	0.004
		100	In situ	I	23.0	------	145.0	-----	1.6	5.8
				R	0.159	------	1.000	-----	0.011	0.040
		600	In situ	I	17.0	------	94.0	-----	1.3	8.9
				R	0.181	------	1.000	-----	0.014	0.095
			Scraped scale	I	2.7	------	-------	-----	------	4.2

[a] a_o = lattice parameter in Å (or $\times 10^{-10}$ m).

[b] Results do not correlate with other compositional information on alloy.

[c] t = tetragonal.
m = monoclinic.

[d] I = intensity = $\times 10^{-3}$ count/min of element.
R = intensity ratio = $I/I_{alloy\ base}$.

TABLE VI. - XRD AND XRF DATA ON TD-Ni

(a) XRD data

Exposure temperature		Exposure time, hr	Sample location	Major phases (a)	Minor phases	Trace
°F	K					
2000	1366	600	Scraped scale	NiO a_o = 4.177±0.004 Å	ThO_2	-----
			Spall	NiO a_o = 4.176±0.004 Å	ThO_2	-----

(b) XRF data

Exposure temperature		Exposure time, hr	Sample location	Element characteristic radiation intensity						
				(b)	CrKα	MnKα	FeKα	CoKα	NiKα	ThLα
°F	K									
1400	1033	4	No scale	I	-----	-----	-----	-----	1070.0	2.8
				R	-----	-----	-----	-----	1.000	0.003
2000	1366	600	In situ	I	0.9	-----	-----	-----	935.0	2.8
				R	0.001	-----	-----	-----	1.000	0.003
			Spall	I	1.7	-----	-----	-----	443.0	1.4
				R	0.005	-----	-----	-----	1.000	0.003

[a] a_o = lattice parameter in Å (or $\times 10^{-10}$ m).
[b] I = intensity = $\times 10^{-3}$ count/min of element.
R = intensity ratio = $I/I_{alloy\ base}$.

TABLE VII. - XRD AND XRF DATA ON TD-NiCr

(a) XRD data

Exposure temperature		Exposure time, hr	Sample location	Major phases (a)	Minor phases	Trace
°F	K					
1800	1254	4	Scraped scale	Cr_2O_3	ThO_2	----
		100	Scraped scale	Cr_2O_3	----	ThO_2
		600	Scraped scale	Cr_2O_3	----	ThO_2
2000	1366	600	Scraped scale	Cr_2O_3	----	----
			Spall	Cr_2O_3, spinel $a_o = 8.33 \pm 0.02$ Å	----	----
2200	1478	4	Scraped scale	Cr_2O_3	----	----
		100	Scraped scale	Cr_2O_3	----	----
		600	Scraped scale	Cr_2O_3	----	ThO_2

(b) XRF data

Exposure temperature		Exposure time, hr	Sample location	Element characteristic radiation intensity						
				(c)	CrKα	MnKα	FeKα	CoKα	NiKα	ThLα
°F	K									
1400	1033	4	No scale	I	55.5	-----	------	-----	657.0	2.6
				R	0.084	-----	------	-----	1.000	0.004
1800	1254	4	In situ	I	54.0	-----	------	-----	615.0	2.1
				R	0.088	-----	------	-----	1.000	0.003
		100	In situ	I	76.0	-----	------	-----	490.0	2.4
				R	0.155	-----	------	-----	1.000	0.005
		600	In situ	I	97.0	-----	------	-----	382.0	2.3
				R	0.254	-----	------	-----	1.000	0.006
2000	1366	600	In situ	I	95.0	-----	------	-----	304.0	2.1
				R	0.312	-----	------	-----	1.000	0.007
			Spall[b]	I	12.7	3.4	12.9	-----	10.7	-----
				R	1.187	0.318	1.206	-----	1.000	-----
2200	1478	4	In situ	I	80.5	-----	------	-----	353.0	1.8
				R	0.228	-----	------	-----	1.000	0.005
		100	In situ	I	113.0	-----	------	-----	207.0	1.7
				R	0.546	-----	------	-----	1.000	0.008
		600	In situ	I	116.0	-----	------	-----	166.0	1.8
				R	0.699	-----	------	-----	1.000	0.011
			Scraped scale	I	3.8	-----	------	-----	3.9	-----
				R	0.974	-----	------	-----	1.000	-----

[a] a_o = lattice parameter in Å (or $\times 10^{-10}$ m).

[b] Results do not correlate with other compositional information on alloy.

[c] I = intensity = $\times 10^{-3}$ count/min of element.

R = intensity ratio = $I/I_{alloy\ base}$.

TABLE XIII. - XRD AND XRF DATA ON RA 333

(a) XRD data

Exposure temperature		Exposure time, hr	Sample location	Major phases (a)	Minor phases	Trace
°F	K					
2000	1366	600	Scraped scale	Cr_2O_3, spinel a_o = 8.44±0.02 Å	----------	-----
			Spall	Cr_2O_3, spinel a_o = 8.40±0.02 Å	----------	-----

(b) XRF data

Exposure temperature		Exposure time, hr	Sample location	(b)	Element characteristic radiation intensity						
					CrKα	MnKα	FeKα	CoKα	NiKα	WLα	MoKα
°F	K										
1400	1033	4	No scale	I	52.0	4.5	93.0	22.0	297.0	4.4	5.1
				R	0.175	0.015	0.313	0.074	1.000	0.015	0.017
2000	1366	600	In situ	I	128.0	15.0	27.0	6.5	90.0	1.9	5.4
				R	1.422	0.167	0.300	0.072	1.000	0.021	0.060
			Spall	I	121.0	32.2	12.4	1.6	23.0	-----	-----
				R	5.261	1.400	0.539	0.070	1.000	-----	-----

[a] a_o = lattice parameter in Å (or $\times 10^{-10}$ m).
[b] I = intensity = $\times 10^{-3}$ count/min of element.
R = intensity ratio = $I/I_{alloy\ base}$.

TABLE IX. - XRD AND XRF DATA ON DH242

(a) XRD data

Exposure temperature		Exposure time, hr	Sample location	Major phases (a)	Minor phases	Trace
°F	K					
1800	1254	4	Scraped scale	Cr_2O_3	----------	-----
		100	Scraped scale	Cr_2O_3	----------	-----
		600	Scraped scale	Cr_2O_3	----------	-----
2000	1366	600	Scraped scale	Cr_2O_3	----------	-----
			Spall	Cr_2O_3, spinel a_o = 8.38±0.02 Å	----------	-----
2200	1478	4	Scraped scale	Cr_2O_3	----------	-----
		100	Scraped scale	Cr_2O_3	----------	-----
		600	Scraped scale	Cr_2O_3, spinel a_o = 8.38±0.02 Å	----------	-----

(b) XRF data

Exposure temperature		Exposure time, hr	Sample location	Element characteristic radiation intensity							
°F	K			(b)	CrKα	MnKα	FeKα	CoKα	NiKα	ZrKα	NbKα
1400	1033	4	No scale	I	55.0	-----	10.0	0.5	668.0	-----	2.1
				R	0.082	-----	0.015	0.001	1.000	-----	0.003
1800	1254	4	In situ	I	69.0	-----	9.2	0.5	542.0	-----	2.5
				R	0.127	-----	0.017	0.001	1.000	-----	0.005
		100	In situ	I	60.0	-----	9.0	0.5	585.0	-----	2.5
				R	0.013	-----	0.015	0.001	1.000	-----	0.004
		600	In situ	I	92.0	-----	5.0	-----	350.0	-----	2.6
				R	0.263	-----	0.014	-----	1.000	-----	0.007
2000	1366	600	In situ	I	87.0	-----	4.2	-----	266.0	0.5	2.5
				R	0.327	-----	0.016	-----	1.000	0.001	0.009
			Spall	I	134.3	5.9	2.6	-----	39.8	0.5	0.2
				R	3.374	0.148	0.065	-----	1.000	0.010	0.005
2200	1478	4	In situ	I	94.0	-----	3.3	0.2	238.0	-----	2.3
				R	0.395	-----	0.014	0.001	1.000	-----	0.010
		100	In situ	I	102.0	-----	2.3	-----	173.0	-----	2.1
				R	0.589	-----	0.013	-----	1.000	-----	0.012
				I	68.0	-----	8.2	-----	483.0	-----	6.2
		600	In situ	R	0.141	-----	0.017	-----	1.000	-----	0.013

[a] a_o = lattice parameter in Å (or $\times 10^{-10}$ m).
[b] I = intensity = $\times 10^{-3}$ count/min of element.
R = intensity ratio = $I/I_{alloy\ base}$.

TABLE X. - XRD AND XRF DATA ON BENDEL

(a) XRD data

Exposure temperature		Exposure time, hr	Sample location	Major phases (a)	Minor phases	Trace
°F	K					
2000	1366	600	Scraped scale	Cr_2O_3	----------	-----
			Spall	Cr_2O_3, spinel a_o = 8.35±0.02 Å	----------	-----

(b) XRF data

Exposure temperature		Exposure time, hr	Sample location	Element characteristic radiation intensity						
°F	K			(b)	CrKα	MnKα	FeKα	CoKα	NiKα	ZrKα
1400	1033	4	No scale	I	95.0	7.6	3.0	0.5	463.0	-----
				R	0.205	0.016	0.006	0.001	1.000	-----
2000	1366	600	In situ	I	128.0	2.0	-----	-----	181.0	-----
				R	0.707	0.011	-----	-----	1.000	-----
			Spall	I	124.4	8.2	2.0	0.5	11.2	0.5
				R	11.07	0.732	0.179	0.045	1.000	0.045

[a] a_o = lattice parameter in Å (or $\times 10^{-10}$ m).
[b] I = intensity = $\times 10^{-3}$ count/min of element.
R = intensity ratio = $I/I_{alloy\ base}$.

TABLE XI. - XRD AND XRF DATA ON HASTELLOY X

(a) XRD data

Exposure temperature		Exposure time, hr	Sample location	Major phases (a)	Minor phases (a)	Trace
°F	K					
1800	1254	4	Scraped scale	Cr_2O_3	----------	-----
		100	Scraped scale	Cr_2O_3, spinel a_o = 8.36±0.02 Å	----------	-----
2000	1366	600	Scraped scale	Cr_2O_3, spinel a_o = 8.37±0.02 Å	----------	-----
			Spall	Cr_2O_3, spinel a_o = 8.39±0.02 Å	----------	-----
2200	1489	4	Scraped scale	Cr_2O_3	Spinel a_o = 8.38±0.02 Å	-----
		100	Scraped scale	Cr_2O_3	Spinel a_o = 8.37±0.02 Å	-----
		600	Scraped scale	Cr_2O_3	Spinel a_o = 8.37±0.02 Å	-----

(b) XRF data

Exposure temperature		Exposure time, hr	Sample location	Element characteristic radiation intensity							
°F	K			(b)	CrKα	MnKα	FeKα	CoKα	NiKα	WLα	MoKα
1400	1033	4	No scale	I	56.0	2.7	119.0	11.0	394.0	1.8	20.0
				R	0.142	0.007	0.302	0.028	1.000	0.005	0.051
1800	1254	4	In situ	I	42.0	1.0	118.0	10.0	397.0	1.0	16.0
				R	0.106	0.002	0.297	0.025	1.000	0.002	0.040
		100	In situ	I	73.0	6.5	73.0	6.5	256.0	-----	16.5
				R	0.285	0.025	0.285	0.025	1.000	-----	0.064
		600	In situ	I	110.0	18.0	24.0	2.2	100.0	-----	15.5
				R	1.100	0.180	0.240	0.022	1.000	-----	0.155
2000	1366	600	In situ	I	118.0	17.0	14.0	2.0	63.0	-----	12.0
				R	1.873	0.270	0.222	0.032	1.000	-----	0.190
			Spall	I	141.5	26.9	7.7	0.5	23.9	-----	------
				R	5.920	1.125	0.322	0.021	1.000	-----	------
2200	1478	4	In situ	I	63.5	2.0	61.0	5.9	222.0	-----	16.0
				R	0.286	0.009	0.275	0.027	1.000	-----	0.059
		100	In situ	I	112.0	6.0	18.0	1.7	85.0	-----	15.0
				R	1.318	0.071	0.212	0.020	1.000	-----	0.176
		600	In situ	I	119.0	10.0	14.0	1.4	58.0	-----	11.5
				R	2.052	0.172	0.212	0.024	1.000	-----	0.136
			Scraped scale	I	25.0	3.1	-------	------	7.0	-----	------
				R	3.571	0.443	-------	------	1.000	-----	------

[a] a_o = lattice parameter in Å (or $\times 10^{-10}$ m).
[b] I = *intensity* = $\times 10^{-3}$ *count/min of element.*
R = intensity ratio = $I/I_{alloy\ base}$.

TABLE XII. - XRD AND XRF DATA ON UDIMET 500

(a) XRD data

Exposure temperature		Exposure time, hr	Sample location	Major phases	Minor phases	Trace
°F	K			(a)		
2000	1366	600	Scraped scale	(Ni, Co)O a_o = 4.19±0.01 Å, spinel a_o = 8.10±0.02 Å	-----	-----
			Spall	Spinel a_o = 8.31±0.02 Å	Cr_2O_3	-----

(b) XRF data

Exposure temperature		Exposure time, hr	Sample location	Element characteristic radiation intensity							
				(b)	CrKα	MnKα	FeKα	CoKα	NiKα	TiKα	MoKα
°F	K										
1400	1033	4	No scale	I	7.8	-----	-----	25.0	78.0	-----	1.4
				R	0.100	-----	-----	0.320	1.000	-----	0.18
2000	1366	600	In situ	I	37.0	-----	-----	134.0	433.0	1.0	8
				R	0.085	-----	-----	0.309	1.000	0.002	0.018
			Spall	I	55.1	-----	3.1	54.2	133.0	0.8	-----
				R	0.414	-----	0.023	0.407	1.000	0.006	-----

[a] a_o = lattice parameter in Å (or $\times 10^{-10}$ m).
[b] I = intensity = $\times 10^{-3}$ count/min of element.
R = intensity ratio = $I/I_{alloy\ base}$.

TABLE VIII. - XRD AND XRF DATA ON CHROMEL A

(a) XRD data

Exposure temperature		Exposure time, hr	Sample location	Major phases (a)	Minor phases	Trace
°F	K					
2000	1366	600	Scraped scale	Cr_2O_3, spinel a_o = 8.34±0.02 Å	----------	-----
			Spall	Cr_2O_3, spinel a_o = 8.33±0.02 Å	----------	-----

(b) XRF data

Exposure temperature		Exposure time, hr	Sample location	Element characteristic radiation intensity						
°F	K			(b)	CrKα	MnKα	FeKα	CoKα	NiKα	ZrKα
1400	1033	4	No scale	I	59.0	---	-----	0.5	675.0	0.5
				R	0.087	---	-----	0.001	1.000	0.001
2000	1366	600	In situ	I	44.0	---	-----	0.5	609.0	-----
				R	0.072	---	-----	0.001	1.000	-----
			Spall	I	129.0	3.1	-----	-----	55.9	0.5
				R	2.308	0.5	-----	-----	1.000	0.001

[a] a_o = lattice parameter in Å (or $\times 10^{-10}$ m).
[b] I = intensity = $\times 10^{-3}$ count/min of element.
R = intensity ratio = $I/I_{alloy\ base}$.

TABLE XIV. - XRD AND XRF DATA ON L-605

(a) XRD data

Exposure temperature		Exposure time, hr	Sample location	Major phases (a)	Minor phases (a)	Trace
°F	K					
1800	1254	4	Scraped scale	Spinel a_o = 8.23±0.02 Å, (Co, Ni)O a_o = 4.248±0.004 Å	----------	-----
		100	Scraped scale	Spinel a_o = 8.20±0.02 Å, (Co, Ni)O a_o = 4.240±0.004 Å	----------	-----
		600	Scraped scale	Spinel a_o = 8.25±0.02 Å, (Co, Ni)O a_o = 4.246±0.004 Å	Cr_2O_3, $CoWO_4$	-----
2000	1366	4	Scraped scale	Spinel a_o = 8.26±0.02 Å, (Co, Ni)O a_o = 4.242±0.004 Å	$CoWO_4$	Cr_2O_3
		100	Scraped scale	Spinel a_o = 8.29±0.02 Å	Cr_2O_3, (Co, Ni)O a_o = 4.249±0.004 Å	-----
		600	Scraped scale	Spinel a_o = 8.29±0.02 Å	(Co, Ni)O, $CoWO_4$	Cr_2O_3
			Spall	$CoWO_4$, (Co, Ni)O a_o = 4.249±0.004 Å	----------	-----

(b) XRF data

Exposure temperature		Exposure time, hr	Sample location	(b)	Element characteristic radiation intensity						
					CrKα	MnKα	FeKα	CoKα	NiKα	WLα	MoKα
°F	K										
1400	1033	4	No scale	I	40.0	5.3	9.0	317.0	86.0	24.0	1.0
				R	0.126	0.017	0.028	1.000	0.271	0.075	0.003
1800	1254	4	In situ	I	41.0	9.8	10.0	342.0	57.0	11.0	1.0
				R	0.120	0.029	0.029	1.000	1.167	0.032	0.003
		100	In situ	I	59.0	19.0	11.0	342.0	56.0	12.0	1.0
				R	0.172	0.056	0.032	1.000	0.164	0.035	0.003
		600	In situ	I	74.0	13.0	8.0	219.0	50.0	21.0	1.0
				R	0.338	0.059	0.036	1.000	0.228	0.096	0.005
2000	1366	4	In situ	I	75.0	15.0	10.0	330.0	73.0	15.0	1.0
				R	0.227	0.045	0.030	1.000	0.221	0.045	0.003
		100	In situ	I	77.0	30.0	6.9	190.0	38.0	9.5	1.0
				R	0.405	0.158	0.036	1.000	0.200	0.050	0.005
		600	In situ	I	61.0	3.3	4.9	145.0	40.0	30.0	1.0
				R	0.421	0.023	0.034	1.000	0.276	0.207	0.007
			Spall	I	22.0	4.8	4.8	142.0	33.5	10.0	1.0
				R	0.155	0.034	0.034	1.000	0.236	0.070	-----
			Scraped scale	I	13.5	1.6	2.6	31.0	7.7	10.0	-----
				R	0.435	0.052	0.084	1.000	0.248	0.323	-----

[a] a_o = lattice parameter in Å (or $\times 10^{-10}$ m).
[b] I = intensity = $\times 10^{-3}$ count/min of element.
R = intensity ratio = $I/I_{alloy\ base}$.

"The aeronautical and space activities of the United States shall be conducted so as to contribute . . . to the expansion of human knowledge of phenomena in the atmosphere and space. The Administration shall provide for the widest practicable and appropriate dissemination of information concerning its activities and the results thereof."

—NATIONAL AERONAUTICS AND SPACE ACT OF 1958

NASA SCIENTIFIC AND TECHNICAL PUBLICATIONS

TECHNICAL REPORTS: Scientific and technical information considered important, complete, and a lasting contribution to existing knowledge.

TECHNICAL NOTES: Information less broad in scope but nevertheless of importance as a contribution to existing knowledge.

TECHNICAL MEMORANDUMS: Information receiving limited distribution because of preliminary data, security classification, or other reasons.

CONTRACTOR REPORTS: Scientific and technical information generated under a NASA contract or grant and considered an important contribution to existing knowledge.

TECHNICAL TRANSLATIONS: Information published in a foreign language considered to merit NASA distribution in English.

SPECIAL PUBLICATIONS: Information derived from or of value to NASA activities. Publications include conference proceedings, monographs, data compilations, handbooks, sourcebooks, and special bibliographies.

TECHNOLOGY UTILIZATION PUBLICATIONS: Information on technology used by NASA that may be of particular interest in commercial and other non-aerospace applications. Publications include Tech Briefs, Technology Utilization Reports and Notes, and Technology Surveys.

Details on the availability of these publications may be obtained from:

SCIENTIFIC AND TECHNICAL INFORMATION DIVISION

NATIONAL AERONAUTICS AND SPACE ADMINISTRATION

Washington, D.C. 20546